TotalControl

Advanced integrated supervisory and wind turbine control for optimal operation of large Wind Power Plants

Predictive Wind Field Model

Deliverable no. 3.9

Delivery date: (31.01.2021)
Lead beneficiary: ORE Catapult
Dissemination level: Public

This project has received funding from the European Union's Horizon 2020 Research and Innovation Programme under grant agreement No. 727680

Author(s) information (alphabetical):		
Name	**Organisation**	**Email**
Søren Juhl Andersen	DTU Wind Energy	sjan@dtu.dk
Ampea Karikari-Boateng	ORE Catapult	ampea.boateng@ore.catapult.org.uk
Audrey Bowie	ORE Catapult	audrey.bowie@ore.catapult.org.uk
Peter Greaves	ORE Catapult	peter.greaves@ore.catapult.org.uk
Ander Madariaga	ORE Catapult	ander.madariaga@ore.catapult.org.uk
Elliot Simon	DTU Wind Energy	ellsim@dtu.dk
Gunhild Rolighed Thorsen	DTU Wind Energy	guth@dtu.dk
Niels Troldborg	DTU Wind Energy	niet@dtu.dk

Acknowledgements/Contributions:		
Name	**Name**	**Name**

Document information

Version	Date	Description		
		Prepared by	**Reviewed by**	**Approved by**
1	28/01/2021	Peter Greaves	Ervin Bossanyi	Ervin Bossanyi

This project has received funding from the European Union's Horizon 2020 Research and Innovation Programme under grant agreement No. 727680

Definitions/Abbreviations

Abbreviation	Definition
ASTM	American Society for Testing and Materials
CDS	Central differencing scheme
CFD	Computational fluid dynamics
DEL	Design Equivalent Load
DES	Detached eddy simulations
DLL	Dynamic link library
DOF	Degrees of freedom
DTU	Technical University of Denmark
GPS	Global positioning system
HAWT	Horizontal axis wind turbine
LES	Large eddy simulations
LiDAR	Light Detection and Ranging
NTP	Network Time Protocol
ORE Catapult	Offshore Renewable Energy Catapult
PLC	Programmable Logic Controller
RANS	Reynolds averaged Navier-Stokes
RANS	Radius
SCADA	Supervisory control and data acquisition system
SST	Shear stress transport

This project has received funding from the European Union's Horizon 2020 Research and Innovation Programme under grant agreement No. 727680

TABLE OF CONTENTS

This project has received funding from the European Union's Horizon 2020 Research and Innovation Programme under grant agreement No. 727680

This project has received funding from the European Union's Horizon 2020 Research and Innovation Programme under grant agreement No. 727680

EXECUTIVE SUMMARY

Deliverable 3.9 of TotalControl describes the efforts undertaken to obtain data (both measured and simulated) to validate a predictive wind field model. It covers challenges with obtaining the measured data, and with aligning the 3 different models (aero-elastic codes Bladed and Flex5 and coupled aero-elastic/CFD code Ellipsys3D-AL).

Despite these challenges, the measured and CFD data were able to validate the vortex cylinder model used to predict the rotor plane wind speed.

INTRODUCTION

The optimisation of wind turbine energy yield while reducing turbine loads via lidar assisted control has received a lot of attention recently. To enable this kind of control, knowing the correlation between the rotor effective wind speed and the wind speed preview offered by nacelle or spinner mounted lidar is crucial. Large deviations of assumed correlations may lead to undesirable and unnecessary control actions. This deliverable investigates utilising lidar, and SCADA data, in combination with CFD modelling to show how the wind speeds preview from a spinner mounted lidar can be used to predict the effective rotor plane wind speed.

For Deliverable 3.9 of TotalControl the Offshore Renewable Energy Catapult (ORE Catapult) and Technical University of Denmark (DTU) are creating and validating a Predictive Wind Field model to use with LiDAR assisted control. The Relationship between how models are used in this work to achieve the final goal is shown in Figure 1 below.

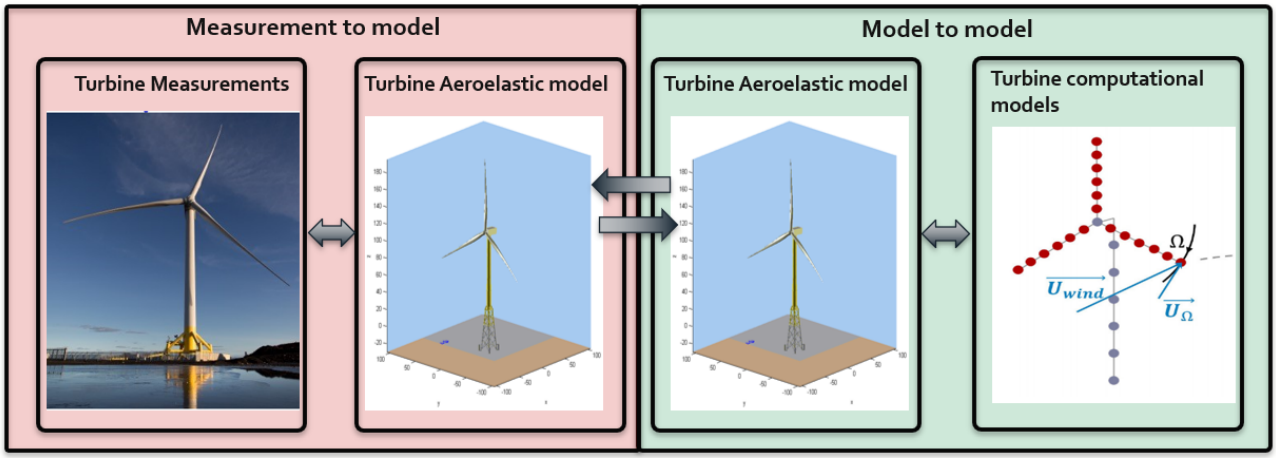

Figure 1 - Relationship between models and data used in this deliverable.

ORE Catapult's role was to gather data from the meteorological mast and supervisory control and data acquisition system (SCADA) of the 7MW Levenmouth Demonstration turbine, and validate the original turbine model created using the aero-elastic simulation tool Bladed by DNV-GL.

DTU's role was to generate turbulent inflow data with the same statistical properties as the measured data to use in the simulation tools. They were also responsible for comparing the results between simulation tools (Bladed, Flex5 and Flex5 coupled to the CFD solver Ellipsys3D-AL), and using the gathered data to validate their model for predicting the advection time.

This project has received funding from the European Union's Horizon 2020 Research and Innovation Programme under grant agreement No. 727680

The data collection exercise is described in section 1, with descriptions of all the sensor equipment which was deployed as part of this task.

Section 2 describes the selection of load cases and how the advection time was estimated from the available data. It also covers an issue faced during the task with the time stamping on the turbine SCADA system. This issue delayed the deliverable considerably because the experimental campaign had to be restarted once this had been fixed.

The generation of representative wind data for the simulation-based aspects of the task is described in section 0. DTU shared .wnd turbulent inflow files with ORE Catapult to allow the Bladed simulations to be performed, with the same data being used for the Flex5 simulations.

Section 0 covers the numerical simulations, including alignment of the Flex5 and Bladed models and the coupled simulations with Flex5 and Ellipsys3D-AL. A comparison is performed between the measured data and the 3 simulation approaches.

Finally, in section 4 the vortex cylinder model used to estimate the advection time is described and the estimates it provides are compared with the measured data and the results from the CFD simulations.

1. Data Collection

Three sets of data are being compared in this report – data from the meteorological mast, data from turbine measurements and data from the forward and rear-facing LiDAR systems. The positions of these data sources are shown in Figure 2 (the LiDAR scan is variable, but its distance was fixed to 120m for the cases described in this report. As the focal point is fixed, the scan describes a spherical cap). The rear-facing LiDAR is also aligned to the turbine, but it has a much longer scan range (up to 2 km), so it could not be shown in this figure.

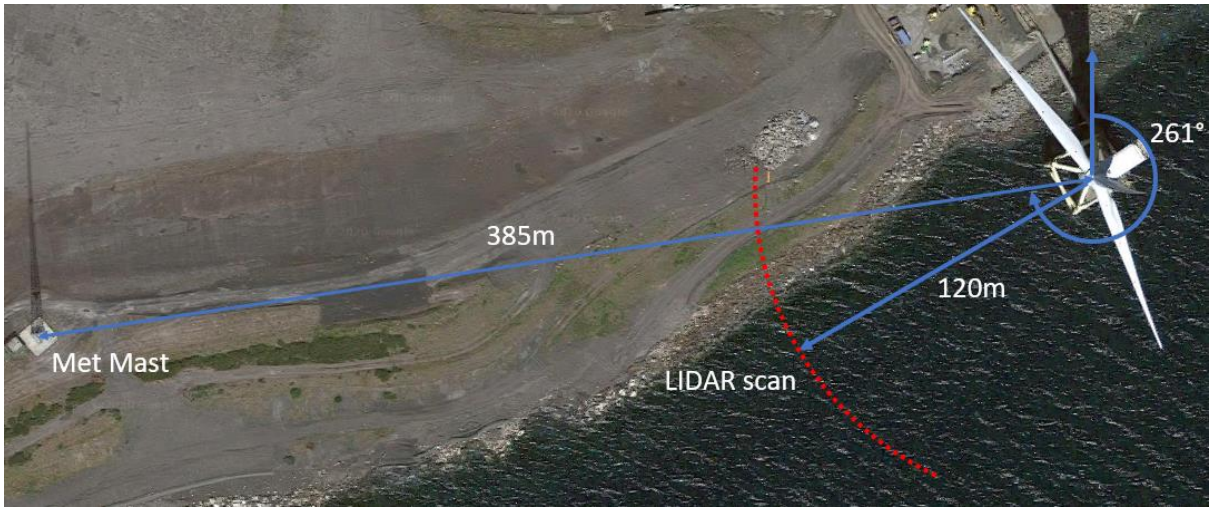

Figure 2 - Distance and orientation of the meteorological mast, turbine, and spinner LiDAR

This project has received funding from the European Union's Horizon 2020 Research and Innovation Programme under grant agreement No. 727680

1.1. Meteorological Mast

The meteorological mast is shown in Figure 3 and Figure 4 – it is equipped with a variety of sensors which record at 1Hz, which are summarised in Table 1.

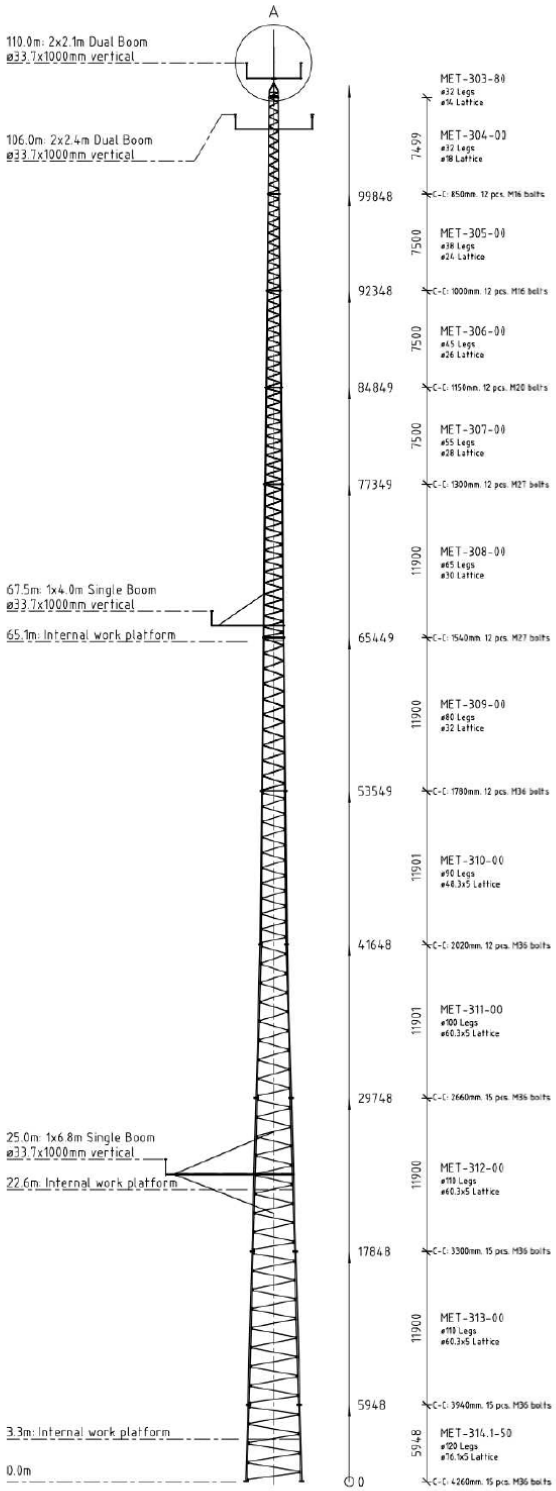

Figure 3 - Meteorological mast

This project has received funding from the European Union's Horizon 2020 Research and Innovation Programme under grant agreement No. 727680

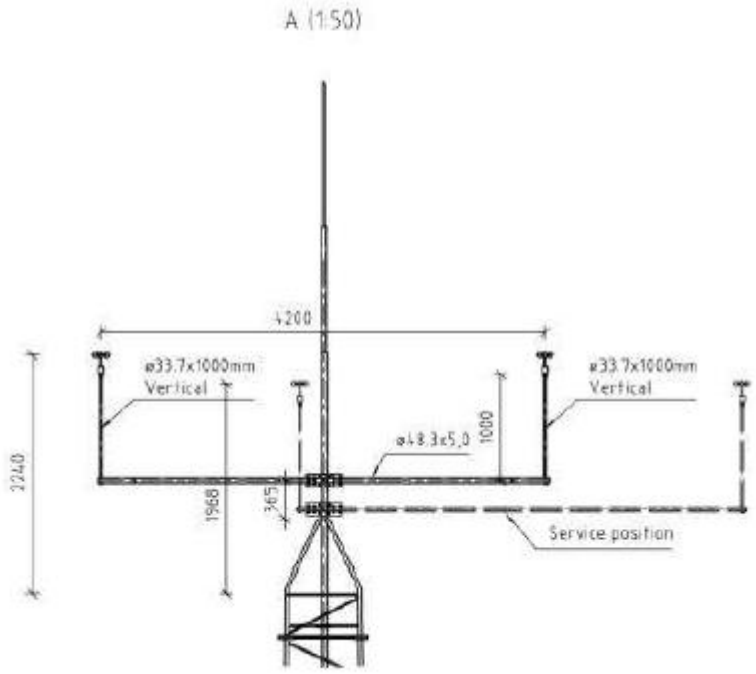

Figure 4 – Detail of Meteorological mast hub height sensors

Table 1 - Meteorological mast channel names

Channel Name	Units	Type	Height	Angle from North
Barometer_2	mBar	Pressure	-	-
Barmoeter_1	mBar	Pressure	-	-
temp_2	degC	Temperature	3m	-
temp_1	degC	Temperature	106m	-
WindVane_2	degN	Wind direction	108m	325°
WindVane_1	degN	Wind direction	108m	145°
Anemo_4	m/s	Windspeed	25m	201°
Anemo_3	m/s	Windspeed	67m	201°
Anemo_2	m/s	Windspeed	110m	307°
Anemo_1	m/s	Windspeed	110m	127°
temp_T	degC	Turbine Temperature	Turbine Nacelle	
WindVane_T	degN	Turbine Wind direction	Turbine Nacelle	
Anemo_T	m/s	Turbine Windspeed	Turbine Nacelle	

This project has received funding from the European Union's Horizon 2020 Research and Innovation Programme under grant agreement No. 727680

1.2. Wind Turbine SCADA

The turbine is also equipped with a supervisory control and data acquisition (SCADA) system which captures 573 channels of data, also at 1Hz. Of these channels, the ones described in Table 2 are of particular relevance for model validation.

Table 2 - Turbine SCADA channel names

Channel Name	Units	Description
Power_kW	kW	Active Power
WindSpeed_mps	m/s	Windspeed
Pitch_Deg	Deg	Blade Pitch Angle
RotorSpeed_rpm	RPM	Rotor Speed
NacelleOrientation_Deg	deg	Direction of nacelle relative to north
YawError3	deg	Yaw error 3. Zero facing into the wind
YawError2	deg	Yaw error 2. Zero facing into the wind
YawError1	deg	Yaw error 1. Zero facing into the wind
WindSpeed3	m/s	Windspeed from Anemometer
WindSpeed2	m/s	Windspeed from Anemometer
WindSpeed1	m/s	Windspeed from Anemometer
RotorPosition	deg	Rotor Encoder Position (IPC)
SubPtchPosition3	deg	Actual Pitch Position Blade 3
SubPtchPosition2	deg	Actual Pitch Position Blade 2
SubPtchPosition1	deg	Actual Pitch Position Blade 1
SubBldLdsOemOutOfPlaneMoBld3	Nm	In plane moments Blade 3
SubBldLdsOemOutOfPlaneMoBld2	Nm	In plane moments Blade 2
SubBldLdsOemOutOfPlaneMoBld1	Nm	In plane moments Blade 1
SubBldLdsOemInPlaneMoBld3	Nm	In plane moments Blade 3
SubBldLdsOemInPlaneMoBld2	Nm	In plane moments Blade 2
SubBldLdsOemInPlaneMoBld1	Nm	In plane moments Blade 1
SubBldLdsPrivOemBld3FwsMo	Nm	Flapwise moment Blade 3
SubBldLdsPrivOemBld3EwsMo	Nm	Edgewise moment Blade 3
SubBldLdsPrivOemBld2FwsMo	Nm	Flapwise moment Blade 2
SubBldLdsPrivOemBld2EwsMo	Nm	Edgewise moment Blade 2
SubBldLdsPrivOemBld1FwsMo	Nm	Flapwise moment Blade 1
SubBldLdsPrivOemBld1EwsMo	Nm	Edgewise moment Blade 1

1.3. LiDAR Systems

Two scanning LiDAR systems were installed on the nacelle roof of the Levenmouth wind turbine in January of 2020 - the forward-facing DTU Spinner-LiDAR [1] and the rear-facing DTU Long-Range WindScanner [2]. A detailed description of the LiDAR measurement methods, data formats, and pre-installation calibration procedures are documented in TotalControl D3.6 [3]. The forward-facing Spinner-LiDAR measured the inflow wind field in front of the turbine rotor, while the rear-facing Long-Range WindScanner measured the wake behind the wind turbine. Processed inflow data was generated following a filtering and reconstruction procedure which produced a single wind vector derived from a combination of the line-of-sight measurements observed across

This project has received funding from the European Union's Horizon 2020 Research and Innovation Programme under grant agreement No. 727680

each scan. This represents the wind speed and direction (relative to the turbine orientation) 120 meters upwind of the rotor every 2-seconds (i.e. a 0.5 Hz sampling rate for the derived wind vector). These processed inflow measurements are used throughout this study to; quality control other reference sensors, select load cases, create an empirical flow advection model, and set up the CFD and aero-elastic simulation input conditions.

2. Load Case Selection

2.1. Load Case Requirements

The selection of representative load cases for Deliverable 3.9 was based on several criteria. It was important to select periods in which the meteorological mast and turbine are aligned with the wind direction, to give a secondary measurement in addition to the spinner LiDAR measurements. It is also necessary to have a variety of different operating conditions – below rated, above rated and around rated speed. Finally, we need a range of different turbulence intensities. These requirements are summarised in Table 3.

Table 3 - Requirements for load cases

	Environment			Turbine operation	
Case	Approximate Average Wind Speed	Wind direction	Turbulence intensity	Pitch angle std-dev	Region
	[m/s]	[°]	[%]	[°]	[-]
1	7.5	261° ±10°	TI <20%	Pt_ang< 0.5	Below rated
2	12.5	261° ±10°	TI <20%	Pt_ang< 1	Around rated
3	18	261° ±10°	TI <20%	Pt_ang > 2	Above rated
4	12.5	261° ±10°	TI > 20%	Pt_ang < 8	Around rated
5	12.5	261° ±10°	TI >25%	Pt_ang< 1	Around rated
6	12.5	261° ±10°	TI > 25%	Pt_ang> 2	Around rated

2.2. Load Case Selection

A script was created using MATLAB to find data files from the SCADA and meteorological mast which satisfied these conditions. As there are almost 150,000 SCADA data files going back three years, the first stage was to filter the files based on the minimum, maximum and average values on all SCADA channels. In addition to the requirements described in Table 3, we also needed to find time periods where the blade load sensors were operational, and they were not working from 18th November '19 until the 15th May '20. This made load case selection more challenging, as the winter/early spring period when stronger winds with higher turbulence intensity were available could not be used. The LiDAR also had to be working properly for any given load case as well.

Figure 5 shows turbulence intensity vs wind speed for the data files where the turbine and met mast were aligned to within 10° and the turbine is producing power - there are 1485 10-minute files between the 15th May and the 18th August '20 where these conditions were satisfied. DTU specified that 20-minute files were preferable, so where two consecutive files satisfied the conditions they were concatenated.

This project has received funding from the European Union's Horizon 2020 Research and Innovation Programme under grant agreement No. 727680

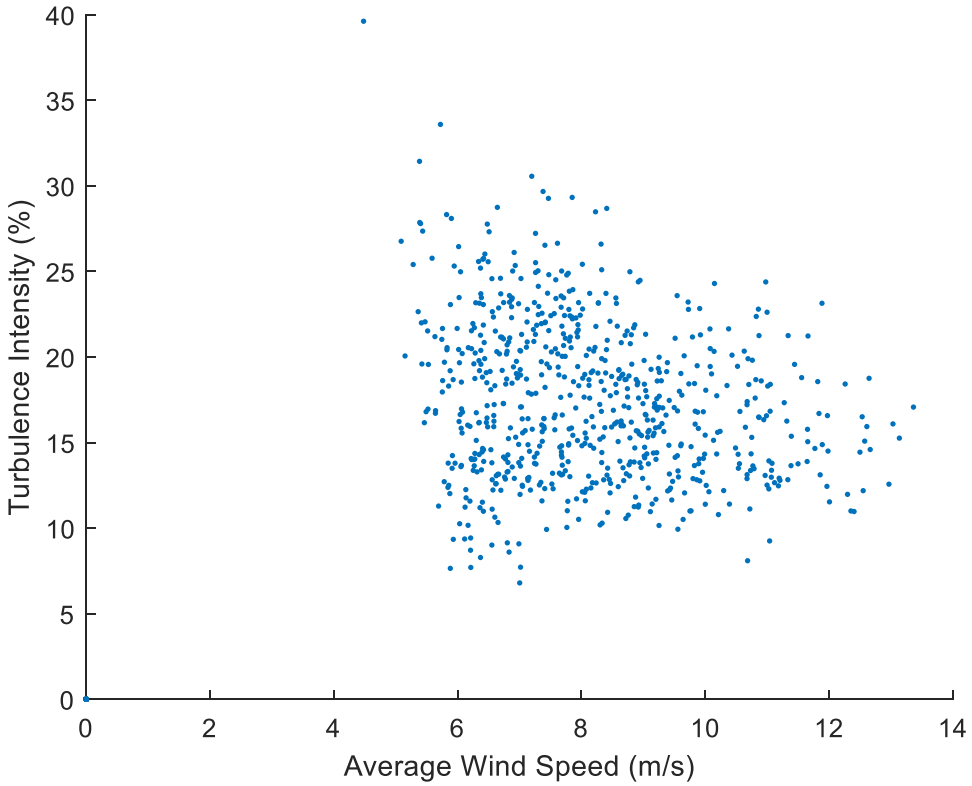

Figure 5 - Wind speed vs turbulence intensity for load cases in which turbine and met mast are aligned

2.3. Determination of Advection Time

This data was then analysed further by finding the time offset between the LiDAR and the nacelle anemometer which maximised the correlation between the two measurements. In practice, this was achieved by offsetting the time of the SCADA wind speed measurement and then interpolating the met mast and LiDAR measured wind speeds at the original time stamps of the SCADA signal. The correlation coefficient for the LiDAR vs SCADA wind speed and met mast vs SCADA wind speeds are recorded for each time offset. Figure 6 shows a plot comparing the correlation coefficients for the two signals. The vertical dotted lines are a simplistic estimate of how long the wind would take to cover the distance from the LiDAR focal point and met mast to the turbine at the mean wind speed from the met mast under a 'frozen turbulence' assumption. Note that in each case, the maximum correlation requires a longer time offset, because the wind is slowed as it approaches the turbine because of induction. The correlation for the LiDAR is far better than that of the met mast because it is much nearer and guaranteed to be aligned with the turbine.

Figure 7 shows the time series for the LiDAR and SCADA wind speed measurements. One point to note here is that the LiDAR has much less variability. This is because the turbine anemometer is operating in the turbine wake, while the LiDAR gives a volume average of the wind speed in the scan plane and the scans are recorded at lower frequency, so there is a time averaging effect as well.

This project has received funding from the European Union's Horizon 2020 Research and Innovation Programme under grant agreement No. 727680

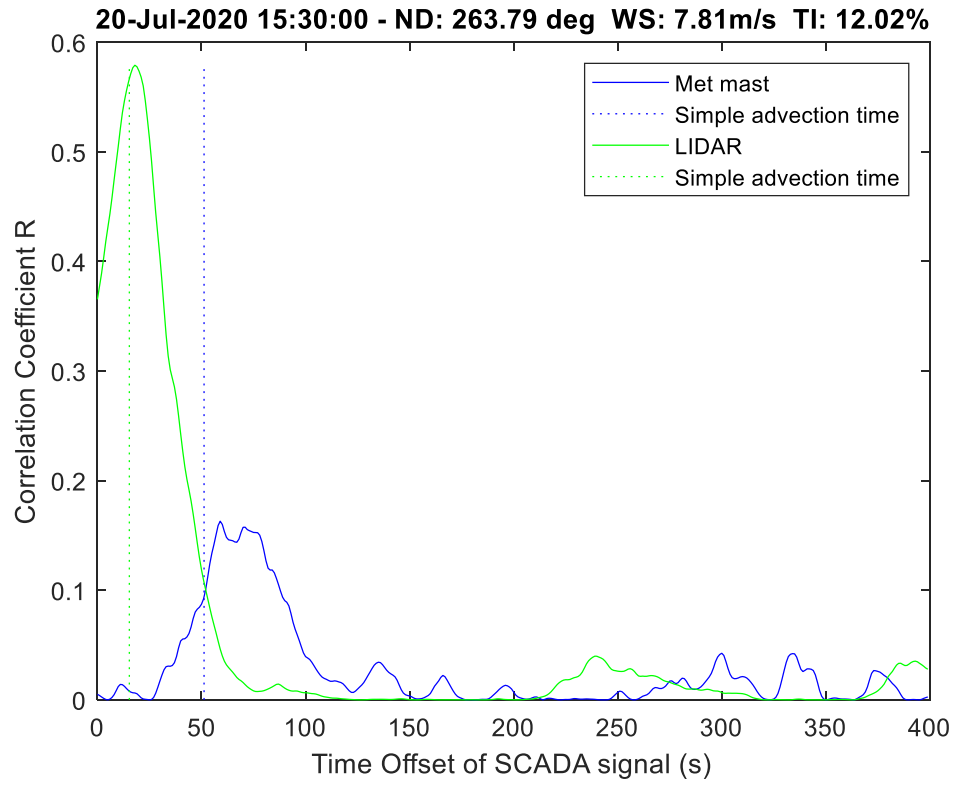

Figure 6 - Correlation coefficient for varying time offsets between SCADA wind speed and LiDAR/ met mast wind speed

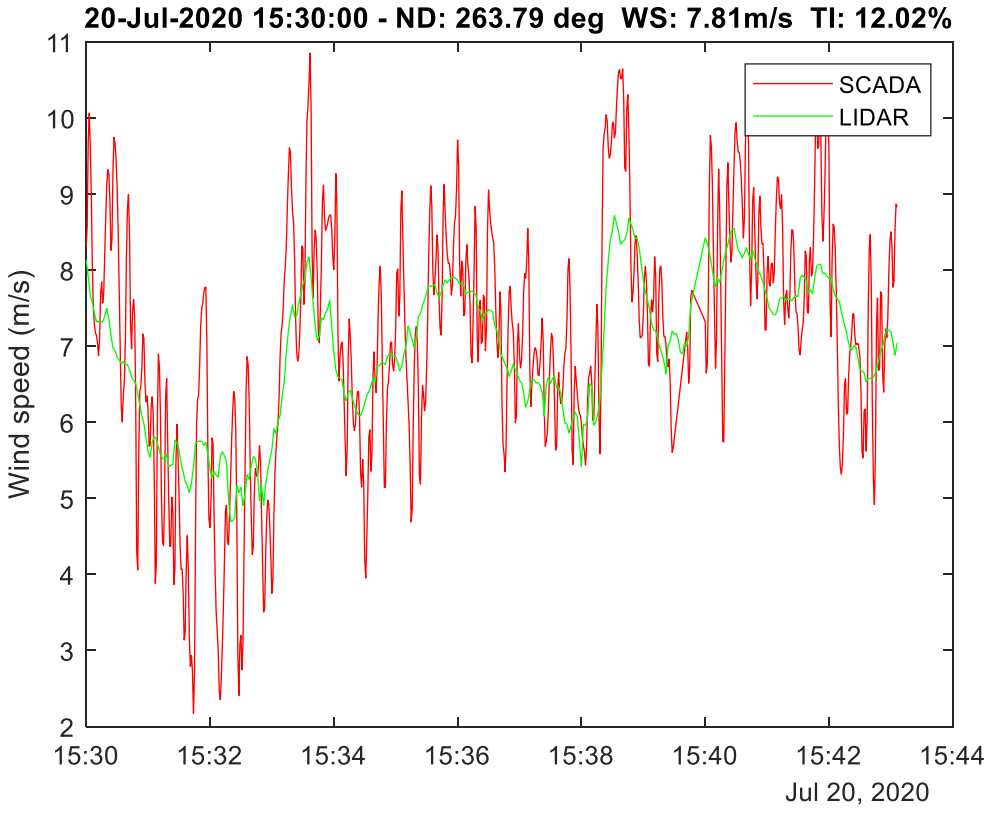

Figure 7 - Aligned LiDAR and SCADA wind speed signals

This project has received funding from the European Union's Horizon 2020 Research and Innovation Programme under grant agreement No. 727680

In order to validate this method of determining the advection time and check which effects were contributing to the correlation, Bladed was used with turbulent inflow which broadly matched the requirements described in Table 3. The results of this exercise are presented in Appendix A.

2.4. SCADA Timestamp Errors

This exercise was performed for all of the 1485 load cases identified in the pre-selection exercise described above (808 cases after concatenation to create longer time series). During this process it was noticed that the advection time for the LiDAR could be up to 5 minutes for many of the data sets – this is impossible given the distance of the focal point to the rotor. An example is shown in Figure 8.

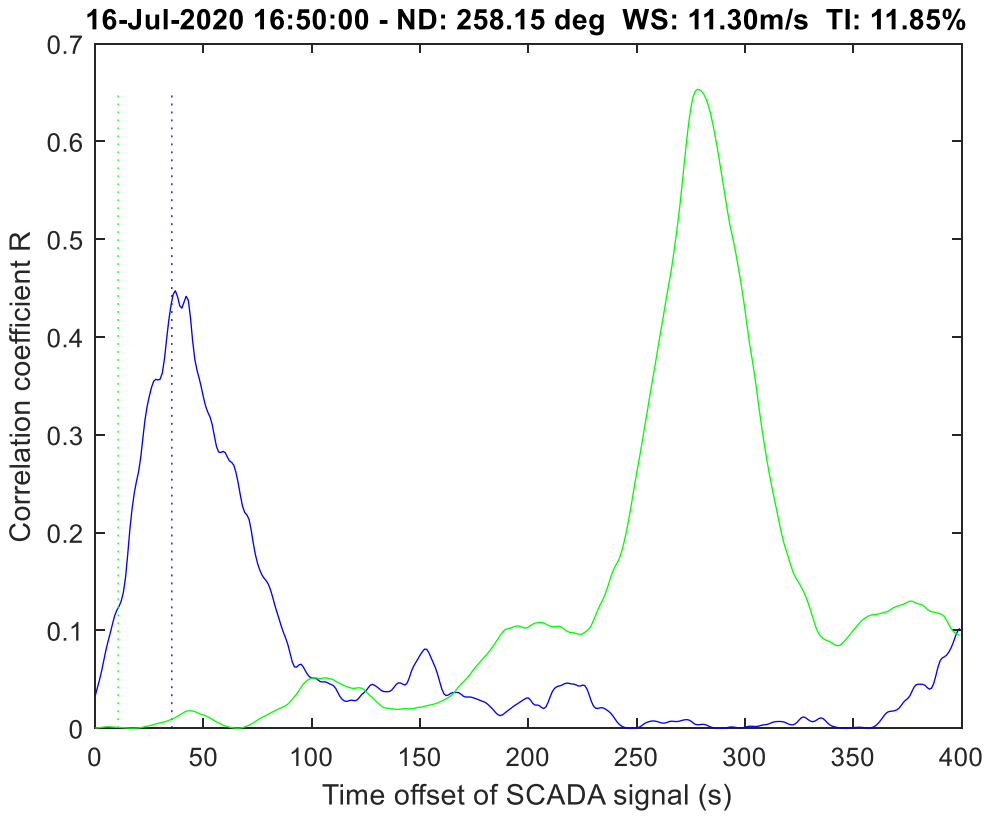

Figure 8- Correlation coefficient for varying time offsets with SCADA clock error

The LiDAR clock is synchronised to Network Time Protocol (NTP) using GPS and was known to be reliable, so as a result of these findings the clock on the SCADA was checked. An error had been discovered on 2nd July '20 by a contractor, so it had been reconfigured to use an NTP time server set up by the ORE Catapult IT department on 20th July '20. Unfortunately, the project team were not made aware of this, so the timestamps were assumed to be reliable for the whole time period.

As a result of a PLC reboot the SCADA clock had gone back to a 4-minute error a few days later. The exact time of the reboot is unknown. The only way to know if the clock is wrong for data from the past is if there is correctly time stamped data to compare against; a check can be done on if it's wrong at the current time by logging into WindHelm and seeing what the clock says. As the LiDAR was down in this period we couldn't tell when it reset. The LiDAR was down for 5 days after

This project has received funding from the European Union's Horizon 2020 Research and Innovation Programme under grant agreement No. 727680

the 22nd of July so there was nothing reliable to compare the SCADA against until 27th July, when the time offset was back. This issue was resolved properly on 20th August.

As this situation only left us with two days of reliable data (during which the wind speeds were quite low) the decision was taken to attempt to determine the time offset to increase the pool of data back to 15th May, when the blade sensors came back online.

This was attempted by using linear regression on all the valid data sets (validity was determined manually based on if there was a clear peak on the correlation plot for a given load case). When the time offset for the data is coloured by load case number there is clear banding as shown in Figure 9, which indicates that the error changes each time there is a PLC reboot. The data with the cyan fitting line is the two days when the clock was correct after the 20th July.

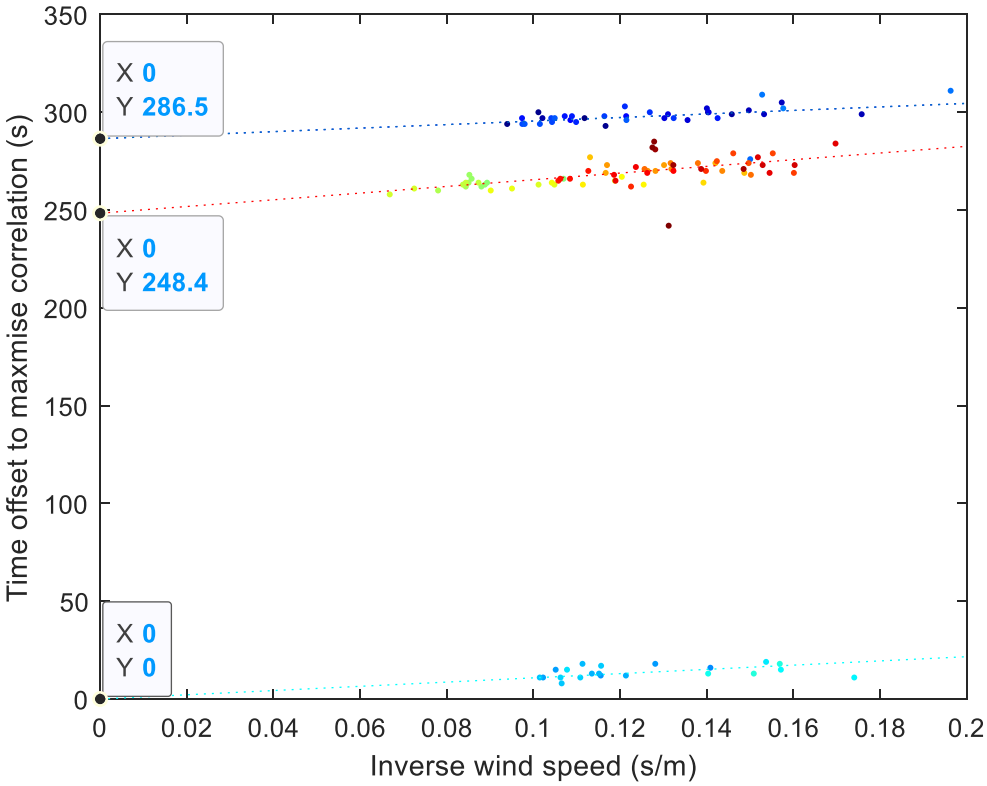

Figure 9 - Attempt to determine timestamp error of the SCADA system

There is a very clear relationship between wind speed and the time offset to maximise the correlation for all three bands. However, the advection time could be as low as 7 seconds for a LiDAR focal point of 120m in a 17m/s wind, so even a 2 second error introduced by attempting to correct for the time stamp would be very significant. For this reason, after discussions with DTU the decision was taken to extend the test program after the 20th August to allow reliable data to be gathered.

This project has received funding from the European Union's Horizon 2020 Research and Innovation Programme under grant agreement No. 727680

2.5. LiDAR Data Wind Speed Offset

As the LiDAR data gets processed according to the method described in [1] there is a volume averaging effect which acts to reduce the turbulence intensity compared to the SCADA and met mast signals. It was also noticed that the LiDAR estimated hub height wind speed tended to be lower than that recorded by the nacelle anemometer, so to see if this was as a result of the way in which data was processed ORE Catapult requested the .spin files (see [3] for a description of these files) from the LiDAR to do further analysis on.

The .spin files are binary files which each contain 46 bytes of data with 12 values logged. Once every scan, a record is created with a special index number that shows the calculated u, v and w velocity components for this scan. This is the value that is logged in the summary data which was used for most of the work.

In order to determine if the offset in measured wind speed was a result of the method used for volume averaging the detailed data from the .spin files was used to check what was happening in the scan region near to the hub height, indicated by the red circle in Figure 10. The tolerance on scans to include in this calculation was S_X and $S_Y < 0.08$. No changes were made to account for the scan angle to the measured velocities in this region, the assumption being that because the angles are small it won't affect the velocity much. The effect of wind shear is clear in Figure 10, and the missed data points near the bottom are where the front of the nacelle and the blades are obscuring the scan.

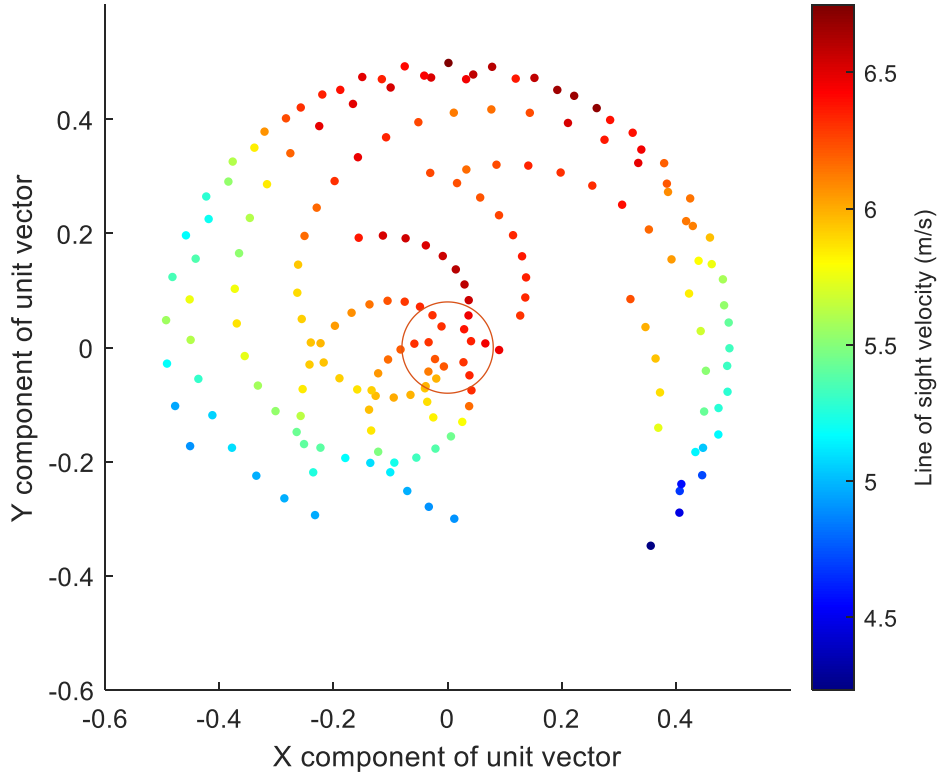

Figure 10 - Line of sight velocity for the whole rotor plane

This project has received funding from the European Union's Horizon 2020 Research and Innovation Programme under grant agreement No. 727680

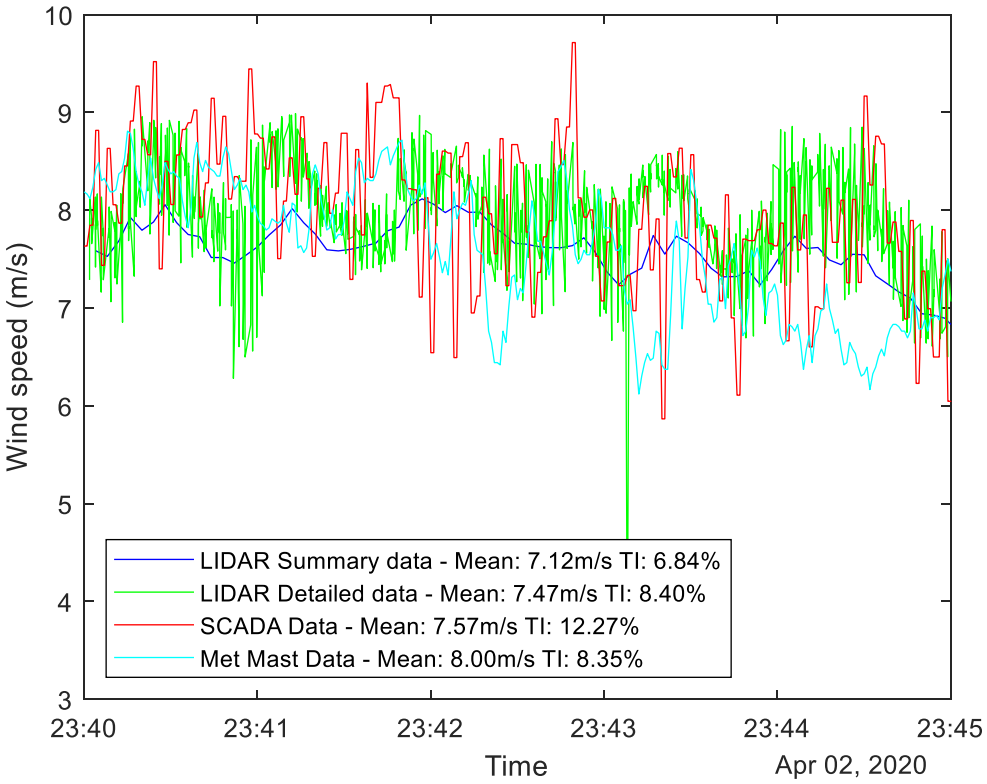

Figure 11 - Comparison for rotor centre area of LiDAR with turbine anemometer (SCADA)

Figure 11 shows the measured wind speed from individual LiDAR scans in the rotor centre in green. The data is noisy because no processing has been performed on it, but it does agree better with the turbine anemometer because the reading is being taken at the hub height instead of being rotor averaged. As the aim of the LiDAR measurement is to obtain a more representative measurement of the wind speed over the whole rotor plane, not just at the rotor centre, the blue line is more accurate overall.

2.6. Data Sets with Correct Timestamps

After the SCADA timestamp issue was resolved, a new dataset consisting of 2765 data files was selected from the period between 20th August and 08th September '20. From this dataset 32 cases were selected, which satisfied the following criteria:

- Wind direction of 261° ± 10° (for all cases below rated wind speed we used 261° ± 5°)
- Yaw error < 5°
- max(NacelleOrientation_Deg) - min(NacelleOrientation_Deg) < 1°
- Power_kW > 0 kW

These criteria ensured that the turbine was operating normally and that the wind direction was aligned with the met mast and turbine. The criteria on limiting the nacelle movement was specified to simplify the comparison with simulations. The mean value of relevant quantities from these cases are summarised in Table 4, in which the wind speed is taken from the nacelle anemometer.

This project has received funding from the European Union's Horizon 2020 Research and Innovation Programme under grant agreement No. 727680

Cases were selected based on the SCADA wind speed and turbulence – the volume/ time averaging effect of the LiDAR gives artificially low turbulence intensity, and the met mast is not necessarily well aligned for all cases.

Table 4 - Summary of selected cases after timestamp issue was fixed

Date and time	Wind Speed	Power	Pitch	Nacelle Angle	Time offset (met mast)	Time offset (LiDAR)	Corr. Coeff. (met mast)	Corr. Coeff. (LiDAR)
	[m/s]	[kW]	[deg]	[deg]	(s)	(s)	(-)	(-)
22/08/2020 21:10	5.09	591	-0.16	251.1	66	19	0.28	0.29
23/08/2020 01:10	8.57	3078	-0.16	256.1	44	14	0.10	0.45
03/09/2020 00:10	11.91	6780	3.14	258.8	32	10	0.32	0.51
03/09/2020 19:20	12.17	6929	3.72	241.4	53	9	0.16	0.57
03/09/2020 18:40	8.78	3539	-0.09	260.3	40	9	0.30	0.51
03/09/2020 19:30	12.28	6871	3.42	241.4	25	9	0.13	0.57
04/09/2020 20:10	10.32	5554	0.87	247.3	48	10	0.08	0.46
04/09/2020 20:20	10.86	6116	1.37	247.3	28	8	0.17	0.54
05/09/2020 17:40	6.15	959	-0.17	247.7	54	14	0.35	0.46
05/09/2020 18:30	8.18	2776	-0.17	253.3	47	6	0.22	0.23
05/09/2020 18:40	7.83	2445	-0.17	253.3	52	14	0.40	0.64
05/09/2020 18:50	7.28	2175	-0.17	253.3	49	12	0.27	0.35
05/09/2020 19:10	8.09	2757	-0.17	249.7	47	14	0.05	0.41
05/09/2020 19:20	8.85	3792	-0.05	249.7	44	13	0.20	0.38
05/09/2020 19:30	7.92	2656	-0.16	249.7	49	12	0.27	0.51
05/09/2020 19:50	8.56	3394	-0.13	256.2	44	14	0.15	0.32
05/09/2020 20:10	8.28	2854	-0.15	256.2	50	11	0.17	0.28
05/09/2020 20:40	8.39	2892	-0.15	256.2	51	11	0.19	0.30
06/09/2020 21:10	6.80	1115	-0.16	252.5	93	19	0.04	0.13
06/09/2020 22:20	6.36	1017	-0.16	244.1	39	30	0.05	0.29
07/09/2020 15:20	14.64	7044	8.50	239.8	49	23	0.06	0.66
07/09/2020 16:20	12.61	4300	8.35	247.5	44	22	0.35	0.11
07/09/2020 17:00	13.48	6942	6.11	240.4	30	22	0.04	0.55
07/09/2020 22:30	9.37	4228	0.16	249.3	50	23	0.17	0.19
07/09/2020 22:40	8.90	3667	-0.07	249.3	49	25	0.27	0.34
08/09/2020 00:00	7.99	2807	-0.15	246.4	55	28	0.07	0.29
08/09/2020 01:50	10.05	4845	0.45	246.8	59	24	0.10	0.35
08/09/2020 02:10	9.81	4693	0.37	246.8	71	24	0.06	0.37
08/09/2020 04:20	8.84	3648	-0.09	244.2	83	27	0.20	0.33
08/09/2020 05:10	8.63	3129	-0.15	249.1	72	27	0.07	0.42
08/09/2020 05:20	7.78	2496	-0.15	249.1	91	28	0.10	0.31
08/09/2020 05:30	8.41	3243	-0.14	249.1	60	28	0.29	0.49

ORE Catapult provided DTU with the meteorological mast measurements described in Table 1 and the turbine SCADA measurements in Table 2 for these cases.

This project has received funding from the European Union's Horizon 2020 Research and Innovation Programme under grant agreement No. 727680

To check the quality of the selected periods, the correlation between the nacelle wind speed and the met mast and LIDAR wind speeds, respectively was analysed to determine the advection speed following the same approach as described in section 2.3.

An example of a case where the fitting has worked well is given in Figure 12 and Figure 13.

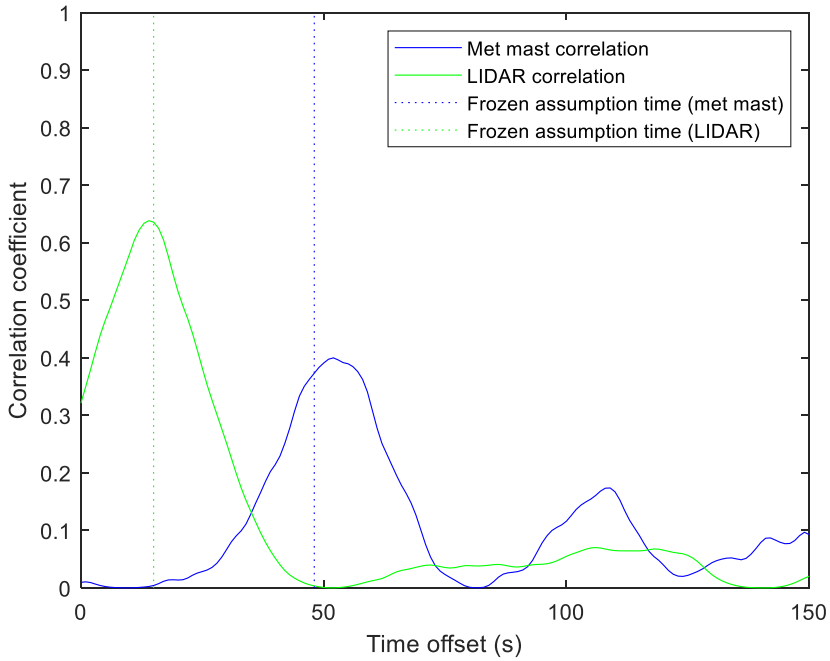

Figure 12 - Correlation by time offset for case 11

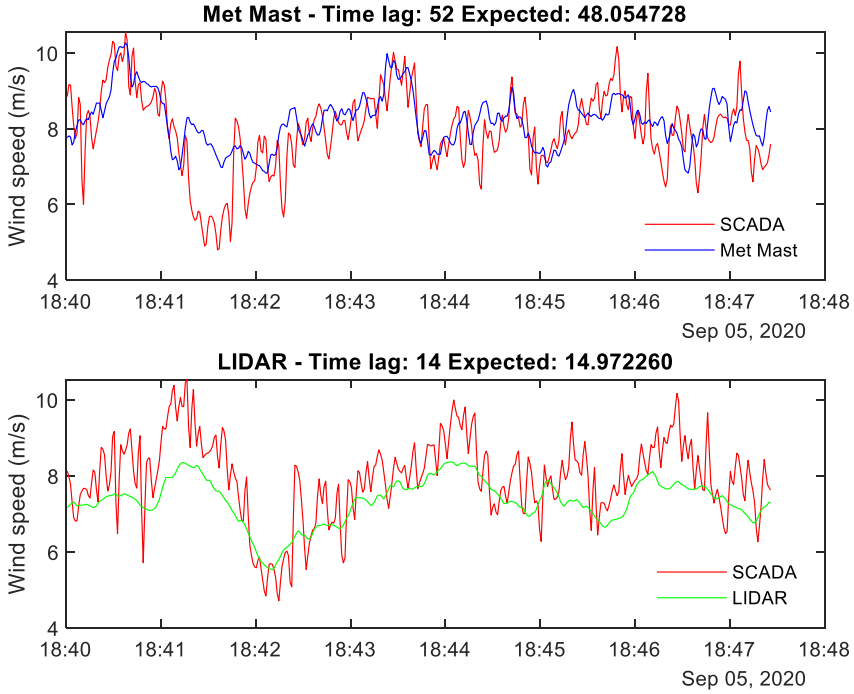

Figure 13 - Offset time histories for met mast and LiDAR for case 11

This project has received funding from the European Union's Horizon 2020 Research and Innovation Programme under grant agreement No. 727680

Not all cases worked this well – there are several examples where the correlation coefficient method failed to find the correct time offset. An example of this is shown in Figure 14 for the meteorological mast, with the resultant time histories in Figure 15.

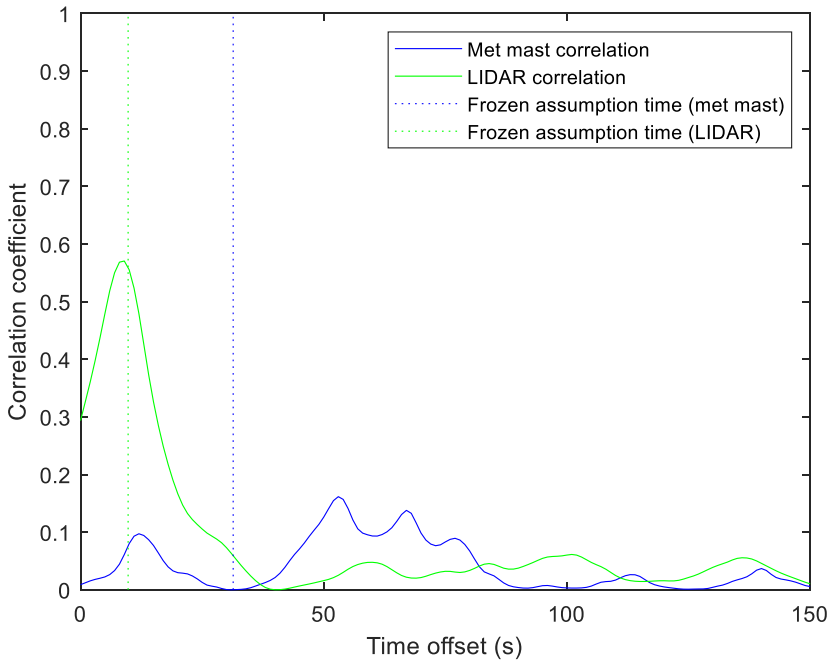

Figure 14 - Correlation by time offset for case 4

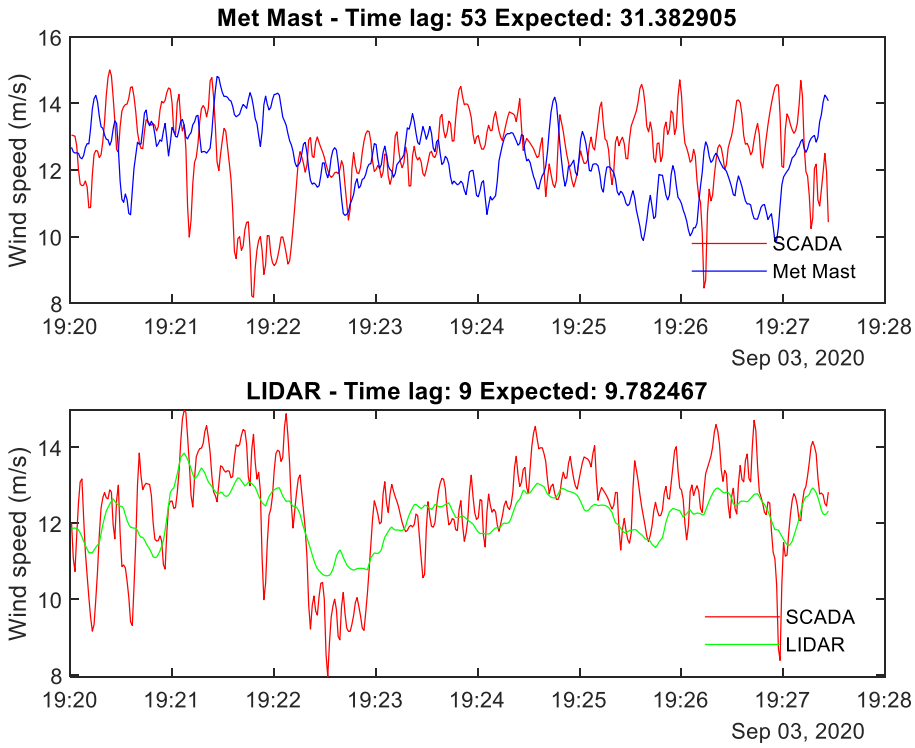

Figure 15 - Offset time histories for met mast and LiDAR for case 4

This project has received funding from the European Union's Horizon 2020 Research and Innovation Programme under grant agreement No. 727680

For this reason, the data was checked manually, and only cases where a sensible time offset and clear correlation were observed were selected. Failure to get the correct offset was mainly caused by a lack of large structures in the data, meaning that there are several peaks in the correlation curve rather than one dominant peak (see the blue line in Figure 14). For the meteorological mast the results for this reduced data set are shown in Figure 16, which shows the determined advection time from the met mast to the turbine against the inverse of the wind speed at the met mast. Linear fits are made to the data, both with and without weighting by the correlation coefficient of the data points. The colour of the data points is the correlation coefficient for that data set, and the advection time for a frozen turbulence assumption is given by the black dotted line for comparison. As DTU are also doing more detailed analysis on the advection model, this information was only generated to check the quality of the results.

For the LiDAR, there is clear banding between results sets as shown in Figure 17. The jump in the time offset occurs on the 6th September between 21:10 and 22:20 (making it unlikely that it was caused by intervention from the turbine maintenance team). The results with data from the period before this jump are shown in Figure 18. The LiDAR scan distance did not change, and there is no evidence of a sudden jump in the wind speed between these times on the SCADA data or meteorological mast data. As the clock on the turbine should have been set by NTP at this point, this has highlighted another possible time stamping issue, which has been passed on to the turbine maintenance team.

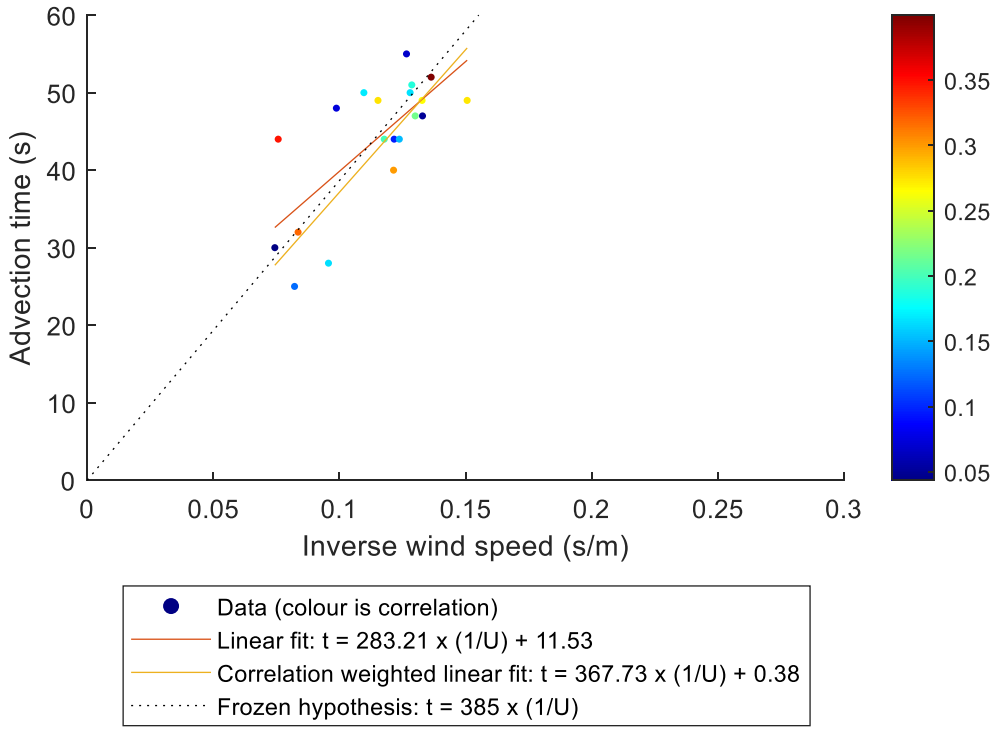

Figure 16 - Advection time fit for meteorological mast

This project has received funding from the European Union's Horizon 2020 Research and Innovation Programme under grant agreement No. 727680

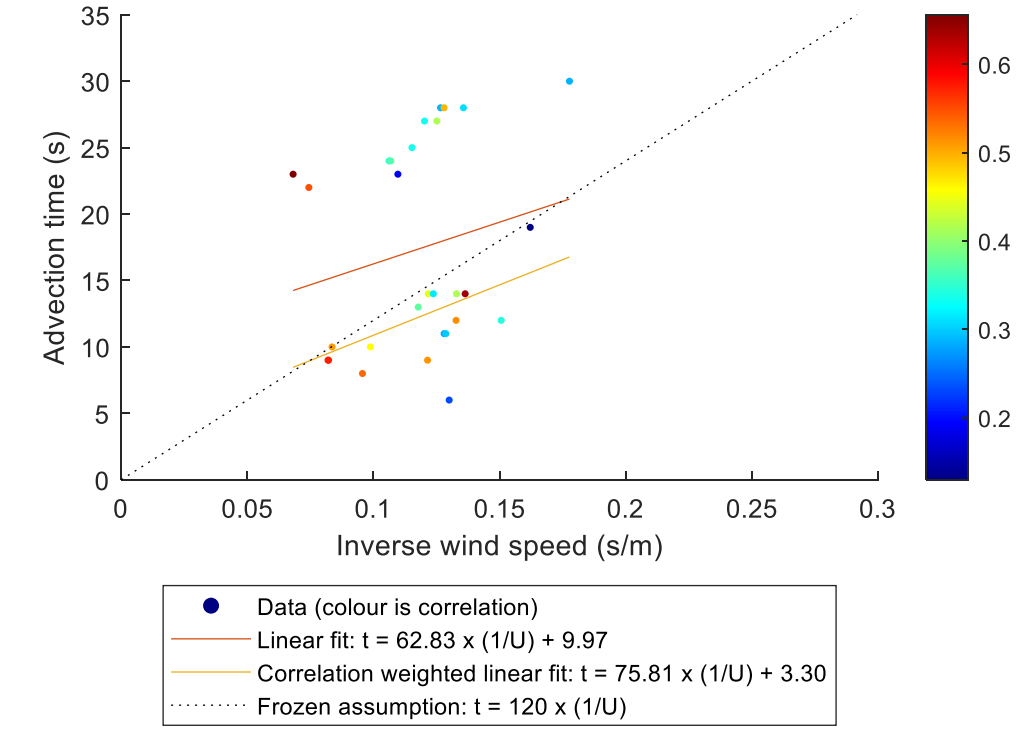

Figure 17 - Advection time fit for the LiDAR (all cases)

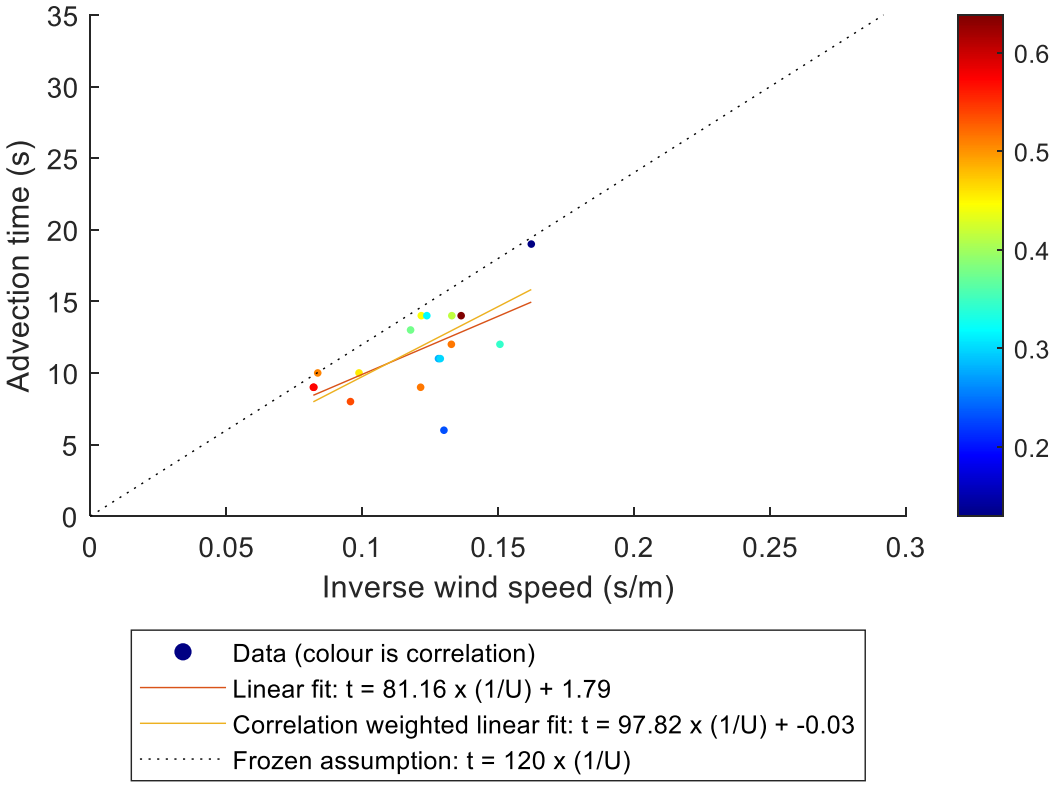

Figure 18 - Advection time fit for LiDAR (cases 1 - 19)

This project has received funding from the European Union's Horizon 2020 Research and Innovation Programme under grant agreement No. 727680

In addition to this table of cases in which the meteorological mast is aligned with the turbine, an analysis was also performed for all the cases in the time period studied (3073 cases, of which 2009 are valid once they've been screened). Figure 19 shows this data, which again shows evidence of banding.

With the data after the jump removed, the data is as shown in Figure 20.This shows that the advection time does not follow one particular relation with the wind speed, but other factors influence the advection time causing it to exhibit wide variations when compared with the wind speed.

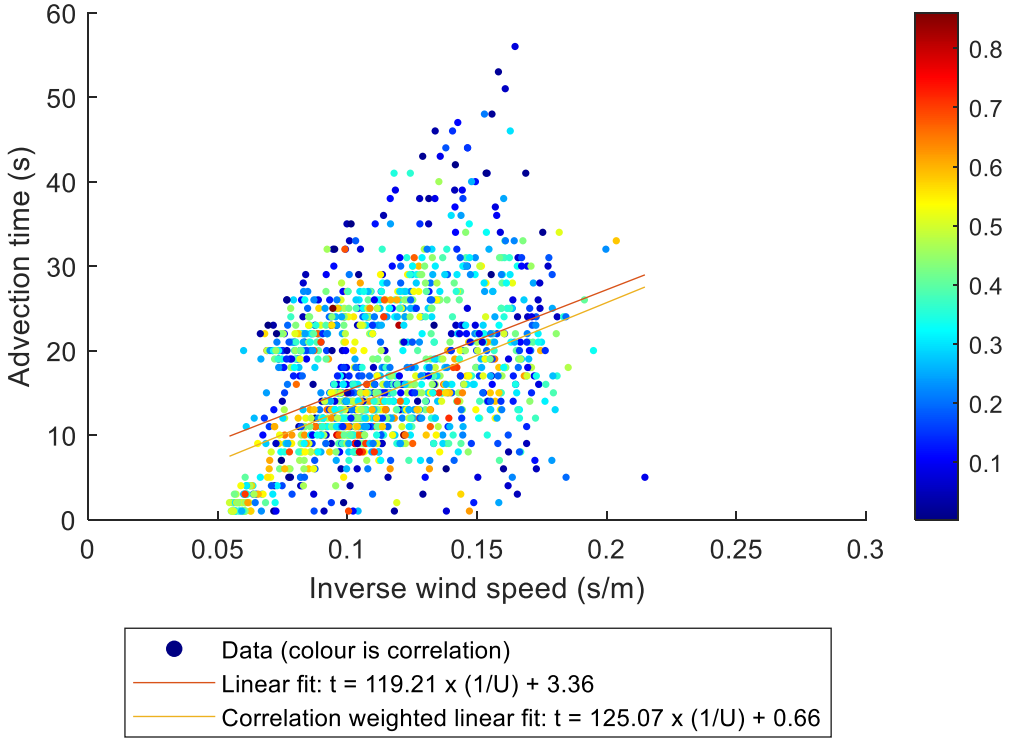

Figure 19 - Advection time determined by maximising cross correlation for all cases

This project has received funding from the European Union's Horizon 2020 Research and Innovation Programme under grant agreement No. 727680

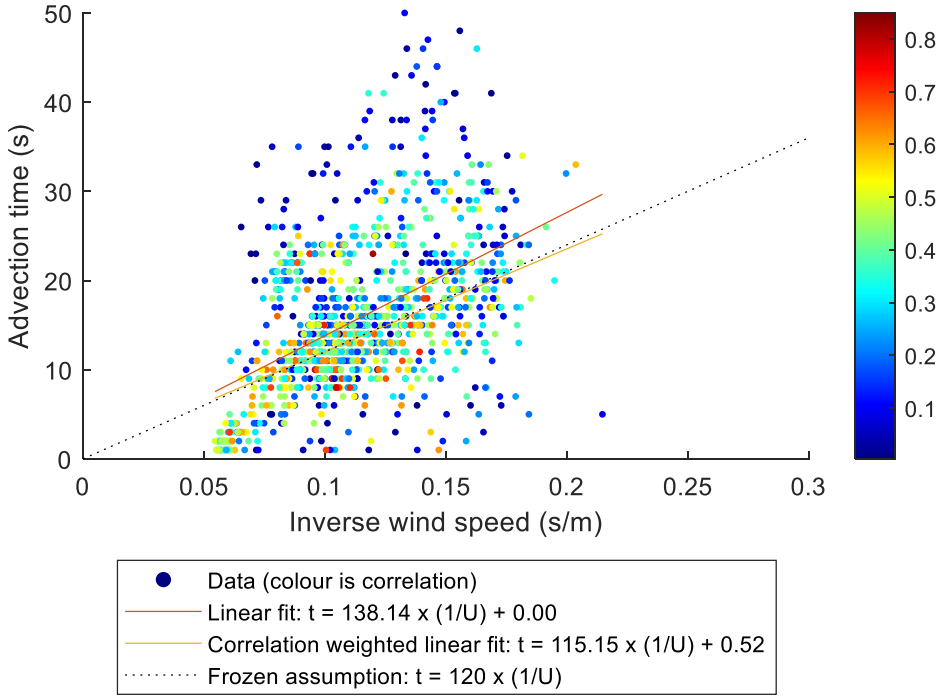

Figure 20 - Advection time determined by maximising cross correlation cases before step in offset was observed

When the data with questionable time offsets was removed from the LiDAR data set, good agreement with the advection time determined using a frozen assumption was found (which was improved further when using the induction model described in section 4). This indicates the data quality was sufficiently high to feed into the later modelling activities.

This project has received funding from the European Union's Horizon 2020 Research and Innovation Programme under grant agreement No. 727680

3. Representative Wind Field Generation

The 32 selected cases were binned on wind speeds with a bin size of 1m/s and thereby categorized into representative wind fields of wind speeds at hub height of 6 m/s, 8 m/s, 9 m/s, 10 m/s, 11 m/s, 12 m/s and 14 m/s, respectively. For each of the 7 representative cases the wind shear was estimated by fitting a logarithmic profile to the mean wind speed at heights 25m, 67m and 110m, respectively

$$u = \frac{u_*}{\kappa} \ln\left(\frac{z}{z_0}\right)$$

From this fit the friction velocity u_* and roughness height z_0 is obtained. The fit resulted in the following estimates of u_* and z_0 for each of the 7 cases: $u_* = [0.86, 0.90, 0.99, 1.13, 1.14, 1.16, 0.96]$ m/s and : $z_0 = [6.0, 3.01, 2.50, 3.01, 3.46, 2.37, 1.58, 0.3]$ m. The roughness heights are surprisingly large which we attribute to the fact that there is a town upstream. Figure 21 (a) shows a representative example of a comparison between the measured mean velocity and the fit - in general the fit is good.

Besides establishing the mean conditions, it is also necessary to generate a representative turbulence field for each of the 7 cases to be used in the subsequent simulations. To do this, a 1-hour turbulence field was generated using the turbulence generator developed by Mann. To resemble the measured conditions, the three parameters as shown in figure 20 governing the spectral tensor in the Mann model are fitted to the measured spectra obtained for wind speeds of $8m/s \pm 1m/s$. Ideally, this fitting should be done on the spectra of all velocity components as well as the cross-spectrum but since only the wind speed is measured at the met mast the fitting procedure can only be done on the stream-wise component. A comparison of the measured and fitted spectrum is shown in Figure 21 (b). The fit is rather good at small and medium length scales but deviates significantly for the larger length scales (small wave numbers). This is partly because the fitting is uncertain when only using one velocity component but could also be because the general assumptions (e.g. neutral atmosphere and homogeneous turbulence) behind the Mann generator are not fulfilled for this site.

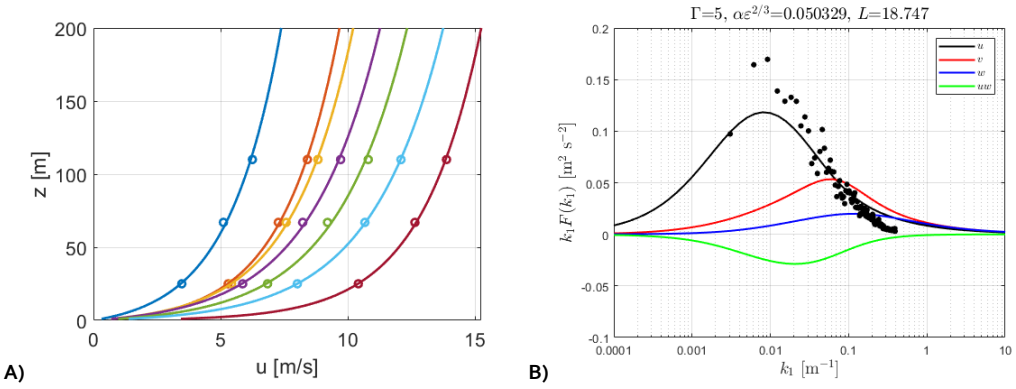

Figure 21 (A) Comparison of Measured and fitted mean velocity profile; (b) Comparison of measured and fitted spectrum

The generated turbulence field was used for all subsequent simulations irrespective of the considered wind speed. Thus, the standard deviation of the turbulence is the same at all

This project has received funding from the European Union's Horizon 2020 Research and Innovation Programme under grant agreement No. 727680

simulated wind speeds. This is not fully consistent with the measurements in which the turbulence level is increasing somewhat with wind speed. The reason for not attempting to account for this increase is partly that the scatter in the measurements is large and because the main part of the available measurements are included in the bin used for estimating the above turbulence spectra.

Numerical Simulations

3.1. Bladed Simulations

In order to validate the turbine model which had been used by DTU to calibrate their Flex5 model, ORE Catapult performed Bladed simulations using the representative wind fields described in section 0.

During this process of alignment between the models, several issues were found with the Bladed model of the Levenmouth turbine which had to be addressed. These included:

- Alignment of the steady state turbine response with the time domain simulations
- Rainflow counting of turbine loads
- Application of correct wind turbine controller
- Updating turbine controller with overridden parameters
- Mismatch between rated power and achieved power

These are described in more detail below.

Like most aero-elastic codes, Bladed can perform steady state calculations to determine quantities such as blade loading and power production. To calibrate the Flex5 model so that it matched the Bladed model and the measurements from the turbine, this process was initially used to determine the relationship between wind speed and power production, rotor speed and pitch angle.

When DTU compared the results between the measured data and the turbine models it was clear that the measured quantities were not agreeing well with the models. The reason for this is that when calculating steady loads Bladed does not use the external controller DLL file which is used for time domain simulations, instead using some basic quantities that maintain the correct generator torque and speed above rated and maximise power below rated, as shown in Figure 22.

This project has received funding from the European Union's Horizon 2020 Research and Innovation Programme under grant agreement No. 727680

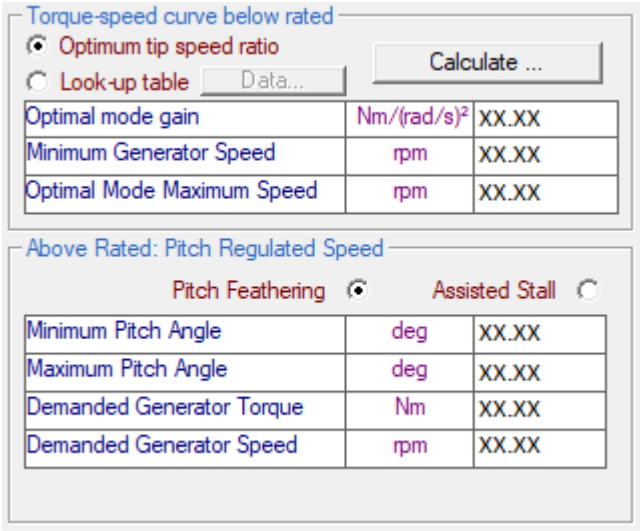

Figure 22 - Bladed Control parameters for steady State Calculations

These quantities were not correct in the model (because of various controller changes since the turbine was commissioned), so to avoid inaccuracies related to the controller time averaged quantities from time stepping simulations with no wind shear or turbulence were used. This method ensured that no errors could be introduced due to the controller (for example from the speed exclusion zone), which would have occurred if the steady curves were used as shown in Figure 23.

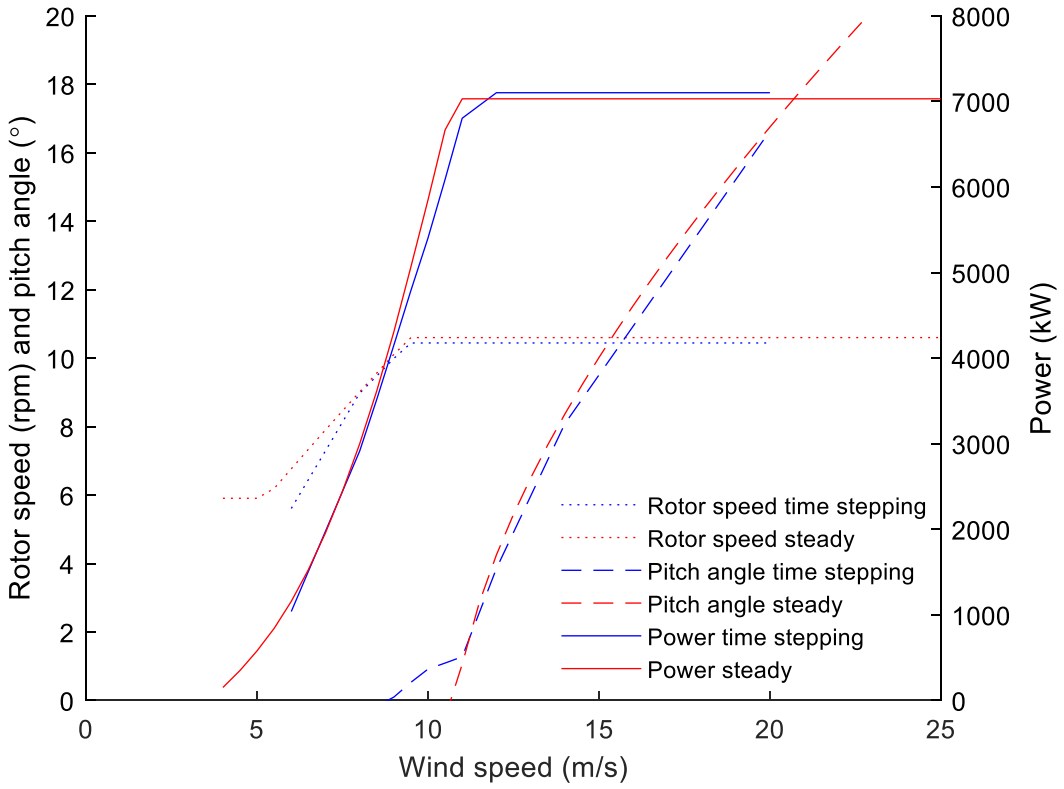

Figure 23 - Comparison of steady vs time stepping control parameter curves

This project has received funding from the European Union's Horizon 2020 Research and Innovation Programme under grant agreement No. 727680

One of the methods of comparing the measured behaviour against the models was using damage equivalent loads (DELs). These are calculated by rainflow counting the time history of the loads, and there are several different methods available.

The ASTM standard [4] method (which is frequently used because it is implemented in a MATLAB script available on the Mathworks File Exchange) does not rearrange the history so that it starts with the largest cycle, which means that it counts half cycles and tends to miss the most extreme cycle. For this reason it is not used for wind turbine calculations, and ORE Catapult sent over a rainflow count according to Downing and Socie [5] which has been validated against the rainflow count in Bladed and is therefore admissible for wind turbine calculations.

Another issue with rainflow counting that can sometimes occur with wind turbine aero-elastic codes is that the data are typically stored as 8 bit precision integers to save file space, which means that in a long time history many data points will have precisely the same values. This can also make rainflow counts invalid and can be easily remedied by importing the data in a higher precision format and adding a very small amount of random noise to it.

Initially the Bladed simulations were performed with the original controller which ORE Catapult had been provided with when the turbine was acquired. When DTU performed comparisons against the measured results with this controller there were clear differences in the pitching schedule and rotor speed, so DNV-GL were contacted to see if they could provide a more up to date controller DLL for the turbine. The new controller still did not resolve the issue, and it became apparent that there were differences in the set points for several parameters in the controller.

These were investigated by creating a Python script which could read the .xml output of a parameter dump from the Bachmann controller on the turbine and compare variables against the values for all the parameters which were also present in the Bladed controller. The result of this was that the generator speed setpoint (amongst several other less important parameters) was found to be different. It transpired that the generator speed had been reduced by Wood Group PLC who manage the turbine because the turbine had stopped due to overspeeds on several occasions.

Another issue which DTU found when comparing against the measured data was that the simulations typically had an average electrical power of 7.1MW when operating above rated, whilst the physical turbine tends to top out at around 6.9MW. Unfortunately, this discrepancy was not resolved during the project because it was only discovered at quite a late stage, but a possible candidate candidate is an errorerror in the definition of the electrical losses. However, we did not want to change the model to match the results without knowing what the true cause of the problem was.

With these issues resolved, the Bladed results were passed to DTU so that they could aggregate the data with the results from Flex5 and Ellipsys3D-AL. These comparisons are presented in section 3.4.

This project has received funding from the European Union's Horizon 2020 Research and Innovation Programme under grant agreement No. 727680

The results were sent as text files containing time histories of the electrical power output, rotor speed, pitch angle for blade 1 and the flapwise and edgewise blade bending moments.

3.2. CFD simulations

The CFD simulations presented in this report are carried out using the Navier-Stokes solver EllipSys3D [6] [7] [8]. EllipSys3D solves the finite volume discretized incompressible Navier–Stokes equations in block-structured general curvilinear coordinates. The simulations are carried out using the detached eddy simulations (DES) model proposed by Strelets [9], which switches from $k-\omega$ SST RANS in the near surface regions to large eddy simulation (LES) in the outer regions.

The coupled momentum and pressure-correction equations are here solved using the SIMPLE algorithm while Rhie/Chow interpolation is used to avoid pressure-velocity decoupling. The convective terms are discretized using a hybrid scheme, which switches between the QUICK scheme in the RANS regions and a fourth-order central differencing scheme (CDS) in the LES regions.

The solution is advanced in time using a second-order three-level implicit time-stepping method with a time step of 0.25 seconds.

The wind turbine is modelled using the actuator disk approach [10] coupled to the aero-elastic tool Flex5 described below.

The simulations are carried out in a Cartesian domain with dimension $(L_x, L_y, L_z) = (25R, 25R, 40R)$ where R = 85.5m is the radius of the turbine and subscript x, y, z denotes the horizontal, vertical and streamwise direction, respectively. The rotor centre is located at $(0,0,0)$. The number of cells in each direction is (N_x, N_y, N_z) = (128,128,384). In the region defined by $-1.25R \leq x \leq 1.25R$, $-0 \leq y \leq 2.75R$, and $-8.5R \leq z \leq 1.5R$ the computational cells are cubic with side length $\Delta = R/32$. Outside of this region the cells are stretched towards the outer boundaries. The boundary conditions are as follows: prescribed velocity at the upstream and top boundaries, zero gradient at the outlet, cyclic conditions at the lateral boundaries and symmetry conditions at the bottom boundary.

The turbulence is inserted in a cross-section 8.25R upstream of the rotor using the method described by Troldborg et al [11]. The turbulence is generated as described above. The turbulence box has dimensions $(L_X, L_Y, L_Z) = (10R, 10R, 316R)$ with a spacing of R/13.

3.3. Flex5 Model

Flex5 is an aeroelastic tool aimed at predicting performance, loads, and deflections of horizontal axis wind turbines (HAWT). Flex5 was developed by Øye [12] and additional details of the framework behind are described in Branlard [13]. In summary, Flex5 is comprised of a BEM method extended with several additional models aimed at modelling the effect of, for instance, yaw, unsteadiness of the wake, and stall over the blades. Flex5 models the turbine using a maximum of 28 degrees of freedom (DOF) with assigned shape functions. Blade torsion is not a DOF in Flex5, which is an important consideration for modelling long and slender blades as is the

This project has received funding from the European Union's Horizon 2020 Research and Innovation Programme under grant agreement No. 727680

case with the Samsung 7MW at Levenmouth. This lack of torsion mainly affected the turbine modelling at and above rated wind speeds and resulted in an almost constant pitch offset above rated. Hence, an additional static twist was applied on the outer part of the blade to counteract this. Figure 24 shows axial and tangential load distributions along the blade for 8m/s, 10m/s, and 14m/s wind speeds for both Flex5 and Bladed. Two Flex5 results are shown, namely the original non-torsional loads and the corrected twist results. Flexible and stiff results are shown for Bladed at 8m/s. As seen, the additional twist yields significant improvements on the load distributions, which match the results from Bladed with flexible blades very well for intermediate wind speeds of 8m/s to 11m/s. The deviations increase for low wind speeds (6m/s) and above 12m/s, but the load distributions remain comparable.

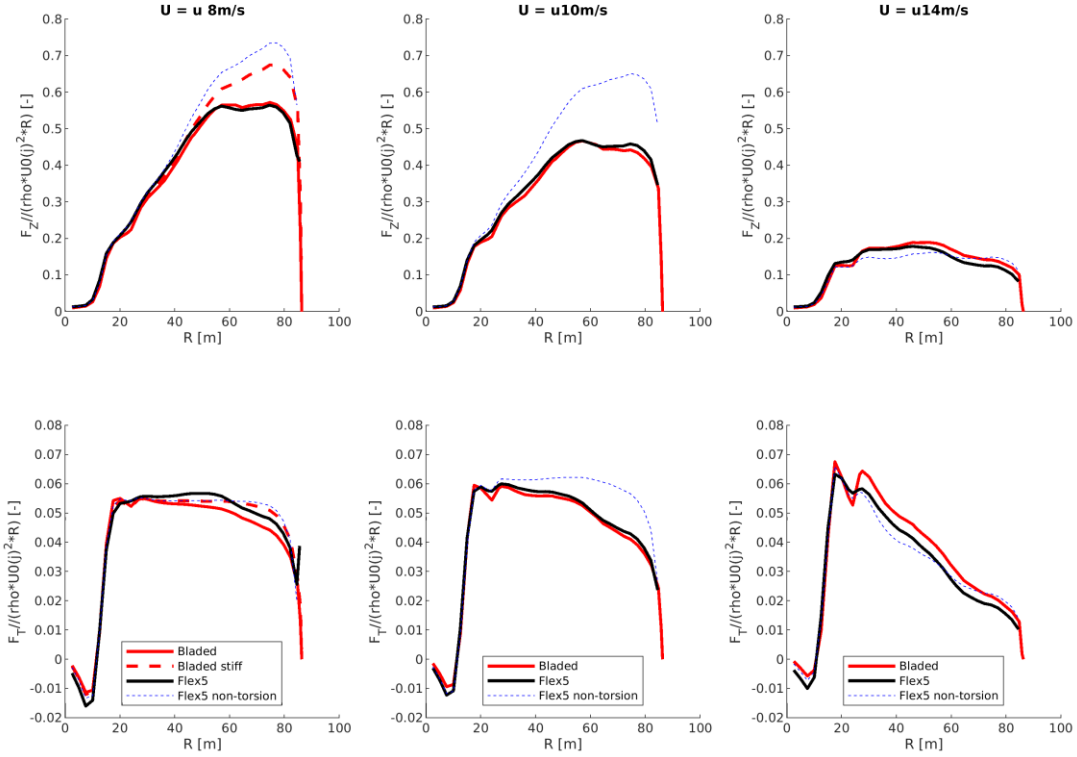

Figure 24 - Normalised axial and tangential load distributions for 8m/s, 10m/s, and 14m/s.

The corresponding steady state power, pitch, and rotational speed curves are shown in Figure 25. The comparison shows very good agreement between the two turbine models, although the slopes of the rotational speed are slightly different, presumably due to some difference in the turbine controller.

This project has received funding from the European Union's Horizon 2020 Research and Innovation Programme under grant agreement No. 727680

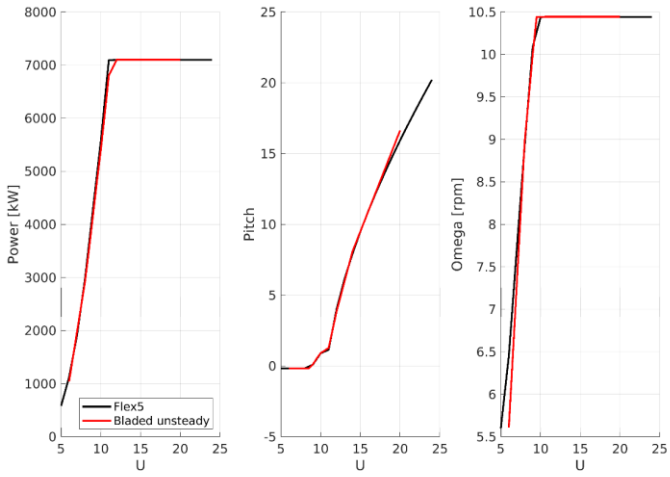

Figure 25 - Steady state power, pitch, and rotational speed curves of Flex5 and Bladed

3.4. Turbine Performance and Damage Equivalent Load Results

The measured turbine performance is compared with model results from the three different sources, namely the LES-AL-Flex5 coupled framework as well as the standalone models of Flex5 and Bladed with turbulent inflow extracted from LES simulations without the presence of the turbine. The instantaneous power, pitch, and rotational speed are shown in box plots for the three model results as well as the experiments in Figure 26, Figure 27 and Figure 28. The dynamics are clearly seen as the boxplots extend widely around the steady state curves, and the model results generally follow the steady state performance. Occasionally, the models do not follow all the performance curve, e.g. increased rotational speed and power for 6m/s and 8m/s. The experimental pitch data generally overlaps with the model results, although it tends to be lower, particularly at higher wind speeds. The experimental rotational speed also shows a significantly larger range than the model results for 9m/s and above, particularly above rated where the rotational speed should be constant. For wind speeds less than 9m/s, the range of rotational speeds experienced by the turbine is significantly reduced compared to the model results, which respond more severely to the dynamic inflow, particularly the Bladed results for 6m/s, which should otherwise have the same controller as the real turbine. A very similar trend is observed in the instantaneous power, where the experimental range is significantly lower at low wind speeds. It is also noteworthy how the turbine appears to be significantly underperforming for all wind speeds. As previously mentioned, the turbine appears to have a maximum power production of approximately 6.9MW although rated power is 7.1MW. Similarly, the full extent of boxplots of instantaneous power production below rated is generally below the steady state curve indicating that the operational performance is statistically different. This is particularly the case for 11m/s, where the turbine is grossly underperforming. These discrepancies can be caused by binning of the experimental data based on the met mast measurements, differences in the modelled flow compared to the flow during the measurements, difference in the controllers, or deterioration of the turbine, e.g. leading edge erosion, which can reduce the turbine efficiency.

It is likely that the cause of discrepancy is that the blade flapwise and edgewise stiffness provided by SSP (originally used in the Bladed 4.2 model) got stiffer towards the tip. This was addressed

This project has received funding from the European Union's Horizon 2020 Research and Innovation Programme under grant agreement No. 727680

with a proper cross-sectional analysis which changed the torsional stiffness by a factor of 1000 at some sections. As the blade is backswept, this could take the angle of attack at the blade tip quite a way off optimal.

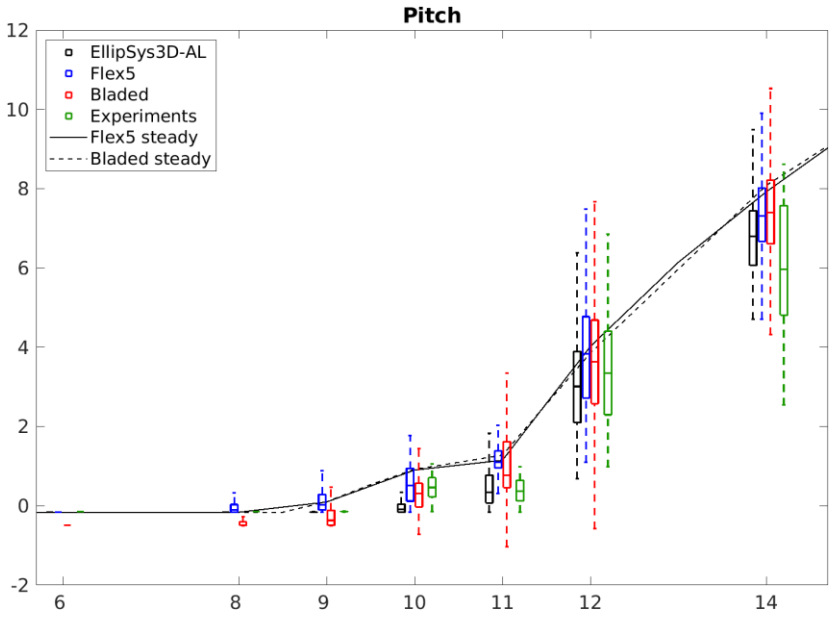

Figure 26 - Boxplots of the instantaneous pitch for EllipSys3d-AL, Flex5, Bladed, and the experiments (the steady state curves are plotted as reference)

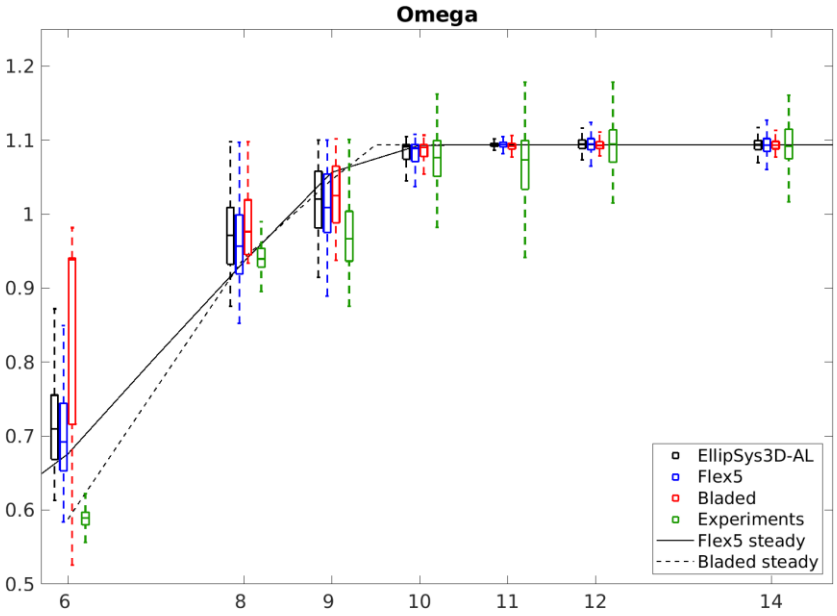

Figure 27 - Boxplots of the instantaneous rotational speed for EllipSys3d-AL, Flex5, Bladed, and the experiments (the steady state curves are plotted as reference)

This project has received funding from the European Union's Horizon 2020 Research and Innovation Programme under grant agreement No. 727680

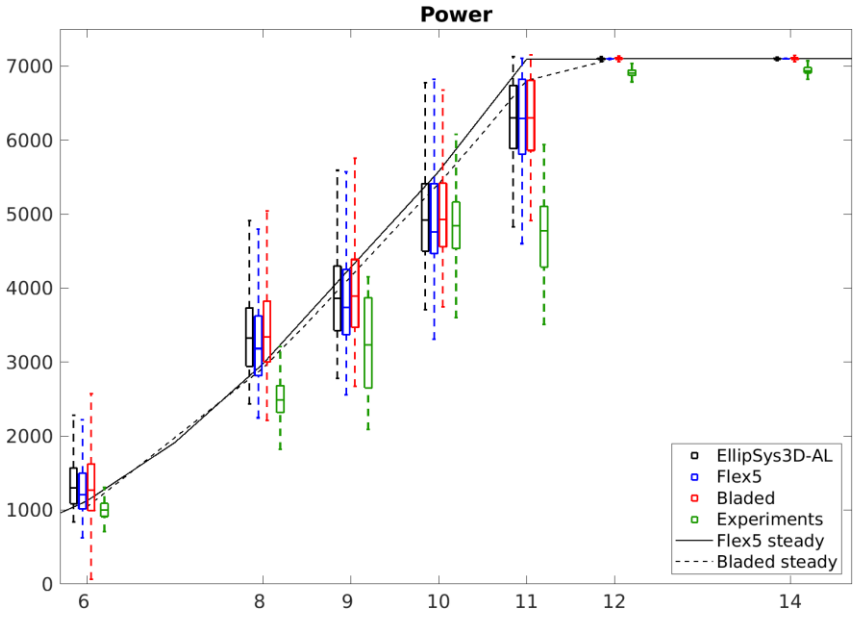

Figure 28 - Boxplots of the instantaneous power for EllipSys3d-AL, Flex5, Bladed, and the experiments (the steady state curves are plotted as reference)

The 10 min 1Hz damage equivalent loads (DEL) are also estimated for flapwise and edgewise root bending moment for all three models and the experimental measurements, as shown in Figure 29 and Figure 30. DELs are included of all three blades in the simulations to show the entire range of DELs during these operating conditions, while the loads have only been measured on a single blade.

Generally, the flapwise DEL tends to increase with increasing wind speed until rated, where the DELs decrease as expected as the turbine starts pitching, thereby reducing the thrust, which is directly correlated with the flapwise root bending moment. All models and the measurements show this trend, but to different degrees.

The DEL of the standalone Flex5 model are seen to have a significantly larger spread than the coupled EllipSys3D-AL results, but otherwise show very comparable medians for most wind speeds. The estimated DEL from Bladed also compares well with Flex5 and EllipSys3D-AL for 8m/s-10m/s, but the DELs are decreased considerably for wind speeds of 11m/s or higher. This could be due to IPC, because actuator constraints in practice limit the amount of IPC action on the turbine. The DTU controller does not include IPC. There might also be a discrepancy in the calibration of the blade load sensors.

Bladed compares very well with the measurements at 9-10m/s with similar medians, but the considerable decrease in DEL for larger wind speeds yields an underestimation in the DEL by Bladed compared to the measurements. The measured DEL are significantly lower than modelled

This project has received funding from the European Union's Horizon 2020 Research and Innovation Programme under grant agreement No. 727680

at 6m/s. Overall, the two estimates by Flex5 compares well to the measured DELs, particularly the standalone Flex5, although the comparison also tends diverge for low wind speeds and at 14m/s.

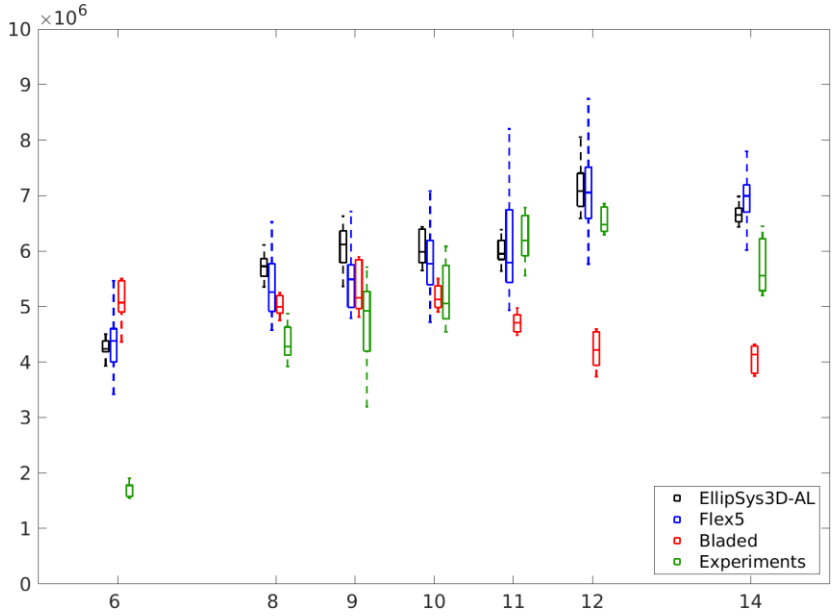

Figure 29 - 10 min Damage equivalent loads Using 1Hz sample of flapwise root bending moment

The corresponding DEL of edgewise root bending moments are shown in Figure 30. Clearly, all estimated DEL remain approximately constant for all wind speeds, as expected since the edgewise root bending moments are largely gravity dominated. The three models show comparable level, but the measured DEL are lower. A possible reason for this is that the blade sensors have a low resolution so the measured values are often exactly the same, in addition to peak lopping caused by the 1Hz data rate being insufficient to fully characterise the shape of the waveform. Both of these factors would contribute to inaccurate DELs. The spread in the standalone Flex5 is essentially non-existing, while both Bladed and EllipSys3D-AL show similar spread in the DEL.

The difference in DEL can be attributed to the difference in the operating conditions, i.e. turbulent inflow realization and the rotor performance in terms of pitch, rotational speed, and power. However, the measured DEL will also depend on the uncertainty of the installed blade strain gauges, as even a minor misalignment or offset will result in a different projection of the loads.

This project has received funding from the European Union's Horizon 2020 Research and Innovation Programme under grant agreement No. 727680

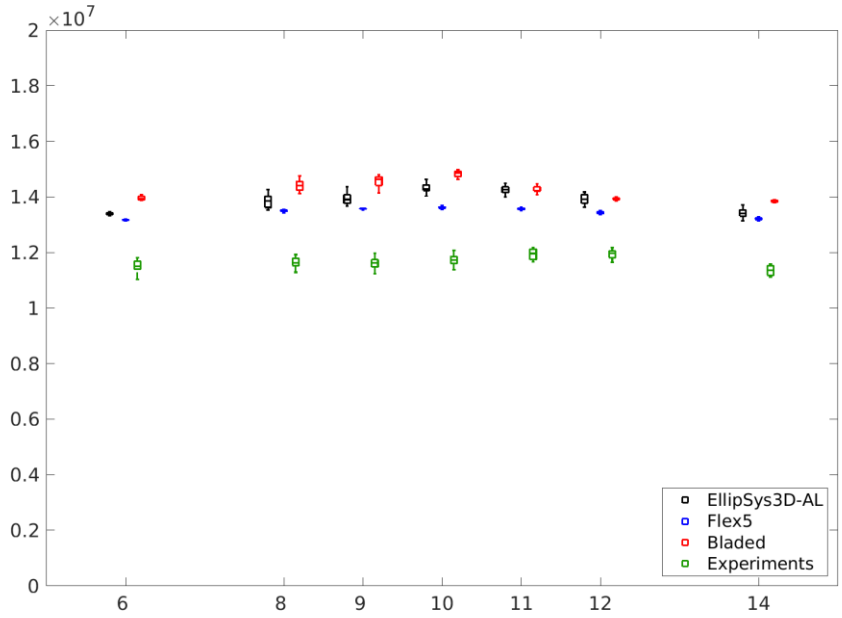

Figure 30 - 10 min Damage equivalent loads Using 1Hz sample of edgewise root bending moment

4. Advection Time Analysis and Model

The advection speed for the turbulence upstream of the turbine is determined from a correlation analysis of the wind speed at the met mast (z=-385 m), the scanning position of the LiDAR (z=-120 m) and at the rotor centre (z=0 m). The advection time between two positions is computed as the time shift, which leads to the maximum correlation of the wind speed at the two positions.

The velocity along the centreline of a rotor can be modelled using a vortex cylinder model (Branlard 2015)

$$\frac{u(z)}{u_\infty} = 1 - a\left(1 + \frac{z}{\sqrt{R^2 + z^2}}\right)$$

Where u_∞ is the free-stream velocity, $a = \frac{1}{2}(1 - \sqrt{1 - C_T})$ is the induction factor and C_T is the thrust coefficient.

The expected time it takes for a particle to move from position A to B along the centreline can then be computed as:

$$\Delta t = \int_A^B \frac{1}{u(z)} dz$$

Combining the two equations above leads to analytical expression for the advection time when the free-stream velocity and thrust-coefficient are known. In the following analysis, we use the thrust coefficient predicted from the steady state Flex5 simulations while the free-stream velocity

This project has received funding from the European Union's Horizon 2020 Research and Innovation Programme under grant agreement No. 727680

is extracted from the met mast. The thrust coefficient is a source of uncertainty but in practice, this uncertainty has only a minor impact on the estimated advection times. This is because the advection times primarily are governed by the free-stream velocity and to a lesser extent on the induction factor. For example the advection time from the LIDAR to the nacelle at C_T=0.8 is only about 3% higher than at C_T=0.88. So even at high thrust a 10% error in C_T results only in a 3% error in the estimated advection time. This sensitivity to thrust uncertainty is even smaller at lower thrust levels as well as when considering advection times from longer distances.

From the measurements and the simulations the following time shifts are computed: Met mast to scanning LiDAR, met mast to wind turbine and scanning LiDAR to wind turbine. The measured advection time shift is based on a subset of the 32 cases described in section 2.6, where the maximum correlation coefficient between the wind speed signals at the met mast, turbine nacelle and scanning LiDAR was greater than 0.5. The CT curve is used from Flex5 for both estimating the simulated and measured advection time. The CT curve is uncertain but in practice does not affect the advection times much because it is an uncertainty on induction which is itself a smaller part of the total velocity

The measured and computed time shifts are then plotted against the time shift expected from vortex cylinder theory. The result is shown in Figure 31.

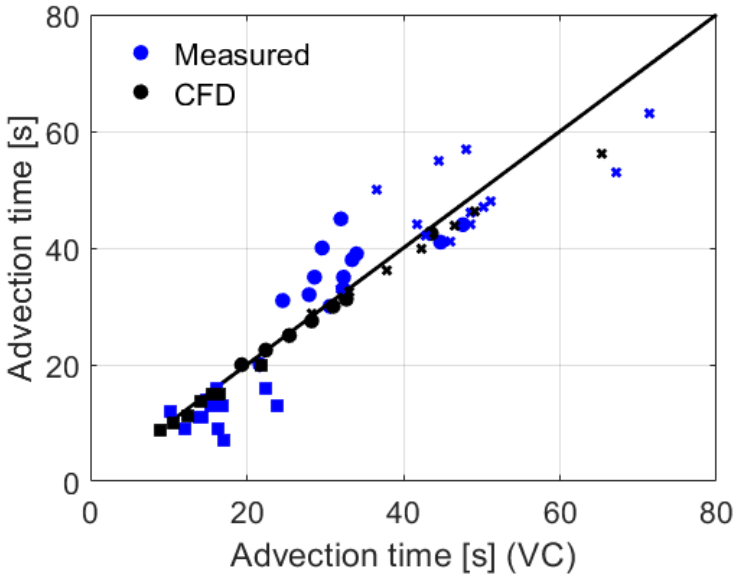

Figure 31 - Comparison of measured and computed advection time against predictions of vortex cylinder theory. Blue markers are measurements and black markers are simulations. Circles are mast to LIDAR, squares are from LIDAR to nacelle and crosses are from mast to nacelle.

As seen the vortex cylinder (VC) theory captures the right trends from both measurements and simulations. The CFD simulations follow the predictions of VC theory quite closely but the VC theory tends to predict higher advection times. This is mainly because VC theory assumes a uniformly loaded actuator disc, while the CFD simulations predict a more realistic span-wise load distribution where the forces near the rotor centre are small. In practice this means that the blockage along the centreline in VC theory is higher than in the CFD simulations. The predictions from measurements are more scattered and at times very large deviations from the VC theory are

This project has received funding from the European Union's Horizon 2020 Research and Innovation Programme under grant agreement No. 727680

observed. The larger scatter in the measurements is attributed to generally lower correlations between the different locations than what is obtained in the simulations. It is a bit unclear what is causing this large scatter in the measurements, but it could be due to general uncertainties in the measurements caused by e.g time-stamp errors or wind speed offsets as described above. During the analysis of the measurements, it was also found that there was an apparent offset of around 10 degrees in the yaw error estimates from the turbine. Although accounted for in the analysis it is yet another source of uncertainty.

5. CONCLUSION

This deliverable has presented the experimental and simulation campaign used to validate a predictive wind field model. Such a predictive model may aid Lidar assisted control by enabling a turbine's controller to utilise lidar measurements taken ahead of a turbine to enhance turbine performance while reducing turbine loads. To carry out the experimental and simulation campaign, several load cases were selected across different control regions of the turbine under normal power production conditions. These covered below-rated conditions, circa-rated conditions, and above-rated conditions.

Initial analysis was conducted for the advection time based on measurements from both the Lidar and Met-Mast by introducing a time shift between the data sets and the turbine's onboard anemometer readings recoded by the SCADA system. A clear advection time was established for some cases as shown in figure 11. Since the lidar is closer to the turbine than the met mast, the advection time closely matches the expected advection time if the flow turbulence is assumed frozen. The Met mast-data tends to correlate less with the SCADA wind speed and the advection time deviates more from a frozen turbulence assumption.

The analysis carried out through measurement gave a good indication of how the flow filed measured in front of a wind turbine via a spinner lidar will evolve into the turbine's rotor plane. It is however challenging to fully understand the flow evolution since measurements are only taken at discrete locations in the flow field.

Computational models allow us to investigate the flow field in more detail because the full significant flow field can be simulated. Several computational models were therefore developed to aid further analysis. The performance of the various turbine models was compared to the experimental measurements in section 0. Common performance indicators such as power production, rotor speed and pitch angles were studied. In addition, the damage equivalent loads of these models were compared with the turbine measurements.

There were reasonable deviations between the turbine models and also between the models and the turbine measurements. It is worth noting however that while the turbine models used similar flow field inputs only their summary statistics match the flow field in the experiments. Consequently, some deviations are expected. Model to model differences were also expected because of differences in the model set up such as the different controllers used.

The advection time analysis and model based on the measurements and computational models in section 4 above showed that, the CFD and turbine measured advection times agreed quite well

This project has received funding from the European Union's Horizon 2020 Research and Innovation Programme under grant agreement No. 727680

with one another but the experimental advection time shows more scatter as expected. For both cases, a good approximation is given by the vortex cylinder model, especially at low advection times. This provides both experimental and computational support for employing the vortex cylinder model to approximate the advection time when using lidar look ahead wind speeds to influence turbine control for load reduction or enhanced performance

This task has highlighted several issues with the data acquisition systems currently used on the 7MW Levenmouth turbine, and also raises some questions about the Bladed simulation modelling. Further work will be necessary to determine if the alignment between measured data and the models can be improved further by amending controller and other parameters.

In addition to the time stamping errors which delayed this deliverable, the measurement campaign was made more challenging by the fact that the met mast is aligned with the prevailing wind direction, which means that there is a town upwind of the turbine for the cases where the met mast could be used for validation.

Despite these challenges, good agreement was achieved between the 3 different simulation models used in this exercise, and the data obtained successfully demonstrated that the vortex cylinder advection model offers a good approximation for the time taken for lidar measured wind speeds to reach a turbine's rotor plane.

This project has received funding from the European Union's Horizon 2020 Research and Innovation Programme under grant agreement No. 727680

6. References

[1] A. Peña, J. Mann and G. Rolighed Thorsen, "SpinnerLidar measurements for the CCAV52," DTU Wind Energy, 2019.

[2] N. Vasiljevic, G. Lea, M. Courtney, J.-P. Cariou, J. Mann and T. Mikkelsen, "Long-Range WindScanner System," *Remote Sensing,* vol. 8, no. 11, p. 896, 2016.

[3] E. Simon, A. Bowie, G. Thorsen, K. Enevoldsen, A. Boateng, C. Stout and J. Richards, "Wind field measurements using LiDAR," DTU Wind Energy, 2020.

[4] ASTM, "ASTM E1049 - 85 (2017) Standard Practices for Cycle Counting in Fatigue Analysis," ASTM, 2017.

[5] S.D.Downing and D.F.Socie, "Simple rainflow counting algorithms," *International Journal of Fatigue,* vol. 4, no. 1, pp. 31-40, 1982.

[6] J. A. Michelsen, "Basis3D – a platform for development of multiblock PDE solvers (Tech. Rep. AFM 92-05)," Dept. of Fluid Mechanics, Technical University of Denmark, 1992.

[7] J. A. Michelsen, "Block structured multigrid solution of 2D and 3D elliptic PDEs (Tech. Rep. AFM 94-06)," Dept. of Fluid Mechanics, Technical University of Denmark, 1994.

[8] N. N. Sørensen, "General purpose flow solver applied to flow over hills (PhD thesis)," Risø National Laboratory, Roskilde, Denmark, 1995.

[9] M. Strelets, "Detached eddy simulation of massively separated flows," in *39th Aerospace Sciences Meeting and Exhibit*, Reno, NV (USA), 2001.

[10] R. F. Mikkelsen , "Actuator Disc Methods Applied to Wind Turbines (MEK-FM-PHD, No. 2003-02)," Technical University of Denmark, 2004.

[11] N. Troldborg, J. Sørensen, R. Mikkelsen and N. Sørensen, "A simple atmospheric boundary layer model applied to large eddy simulations of wind turbine wakes," *Wind Energy,* vol. 17, no. 4, p. 657–669, 2014.

[12] S. Øye, "FLEX4 simulation of wind turbine dynamics," in *Proceedings of 28th IEA meeting of experts concerning state of the art of aeroelastic codes for wind turbine calculations*, Lyngby, 1996.

[13] E. Branlard, "Flexible multibody dynamics using joint coordinates and the Rayleigh-Ritz approximation: The general framework behind and beyond Flex," *Wind Energy,* vol. 22, no. 7, pp. 877-893, 2019.

[14] E. Bossanyi, "Un-freezing the turbulence: application to LiDAR-assisted wind turbine control," *IET Renewable Power Generation,* vol. 7, no. 4, pp. 321-329, 2013.

[15] DNV-GL, "Bladed Theory Manual," DNV-GL, 2020.

[16] DNV-GL, "Bladed User Manual," DNV-GL, 2020.

[17] E. Branlard and M. Gaunaa, "Cylindrical vortex wake model: right cylinder," *Wind Energy,* vol. 11, no. 1973-1987, p. 18, 2015.

This project has received funding from the European Union's Horizon 2020 Research and Innovation Programme under grant agreement No. 727680

APPENDIX A - BLADED SIMULATIONS FOR ADVECTION TIME ANALYSIS

In order to validate the method described in section 2.3 for determining the advection time from the SCADA and LiDAR wind speed data, some simulations were performed using Bladed.

Bladed has some in-built LiDAR patterns which are accessible via the user interface (in addition to being able to program LiDAR paths as part of a controller DLL). The in-built rosette style pattern is different to the DTU spinner LiDAR (see [3]) but for this exercise, the aim was not to accurately capture the LiDAR behaviour so the fact that the scanning pattern was different was not of concern. The LiDAR parameters used are given in Table 5.

If a LiDAR is used to scan ahead of the turbine, then the frozen turbulence assumption which is typically used for simulations is no longer valid, as turbulence evolves over the distance between the scan plane and the rotor plane. Bladed allows the user to specify two turbulent wind files which are identical apart from their random number seeds. The first file is assumed to evolve into the second after a very long time, with the high frequency components evolving more quickly. A more detailed description of the method used is given in [14] and [15].

Table 5 - Bladed Simulations LiDAR parameters

Parameter	Value
Type	Continuous Wave
Lens Area	0.01m^2
Laser Wavelength	1000nm
Focal Distance	120m
Scan Mode	Rosette
Number of lobes	6
Max angle	36°
Min angle	6°
Samples per scan	150
Measurement interval	0.014s

The user must also specify that the LiDAR data captured at the focal point is logged as a measured signal in the control set up.

The load cases described in Table 6 were simulated using the Kaimal turbulence model with default values for turbulence length scales and coherence parameters from IEC 3. These cases roughly correspond to those in Table 3, but the turbine controller will determine the pitch action so case 5 and 6 have been considered to be the same.

This project has received funding from the European Union's Horizon 2020 Research and Innovation Programme under grant agreement No. 727680

Table 6 - Load cases analysed

Load case	Average Wind Speed (m/s)	Turbulence intensity (%)
1	7.5	10
2	12.5	10
3	18	10
4	12.5	22
5	12.5	27

Case 1

Figure 32 shows a comparison of the original time series. The LiDAR leads the turbine signals because it is scanning 120m upwind of the nacelle LiDAR (112m ahead of the hub centre, where the anemometer is assumed to be mounted in Bladed). The original LiDAR signal is much noisier because each sample is at a different point in the rotor area – the signal shown in the plot is the average value over all 150 samples in the scan.

Figure 33 shows the variation in correlation coefficient with time offset. The maximum value of 0.46 is at 15.65s, and the mean wind speed is 7.5m/s for this case. We would therefore expect an advection time of 14.93s (Bladed does not account for induction). If we offset by 15.65s we get the result shown in Figure 34, and the improvement in correlation shown in Figure 35. Clearly the LiDAR underpredicts the hub height wind speed – however, it is supposed to give us a representative wind speed for the whole rotor area.

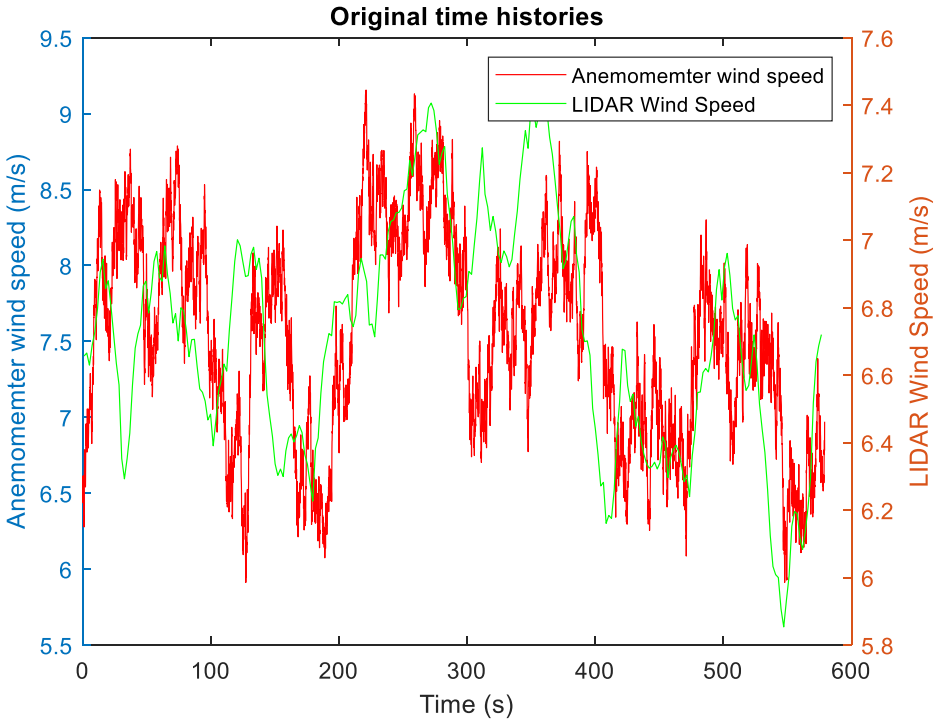

Figure 32 - LiDAR and anemometer wind speeds with no offset

This project has received funding from the European Union's Horizon 2020 Research and Innovation Programme under grant agreement No. 727680

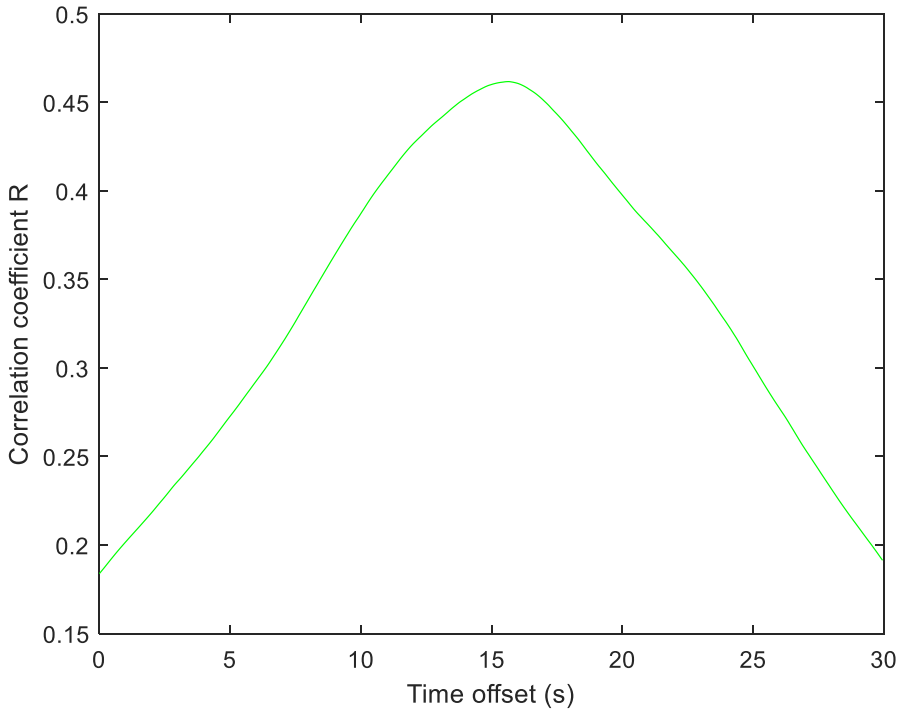

Figure 33 - Variation in correlation coefficient with time offset

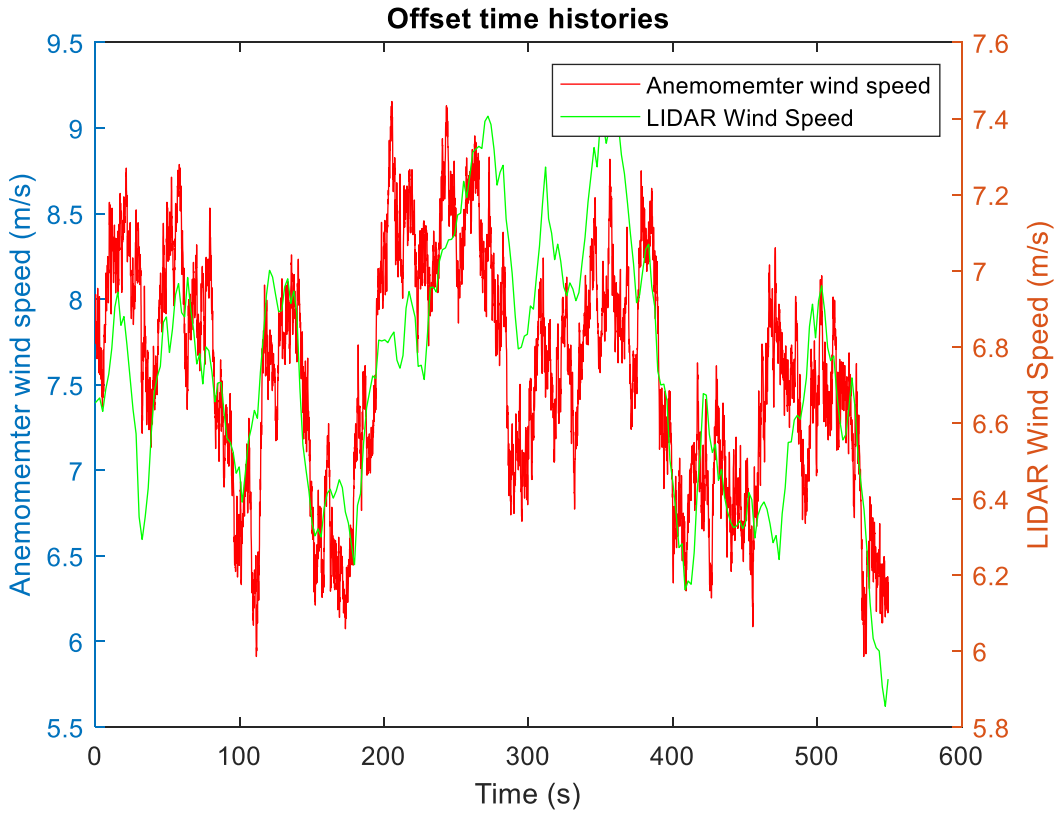

Figure 34 - After the time series have been offset

This project has received funding from the European Union's Horizon 2020 Research and Innovation Programme under grant agreement No. 727680

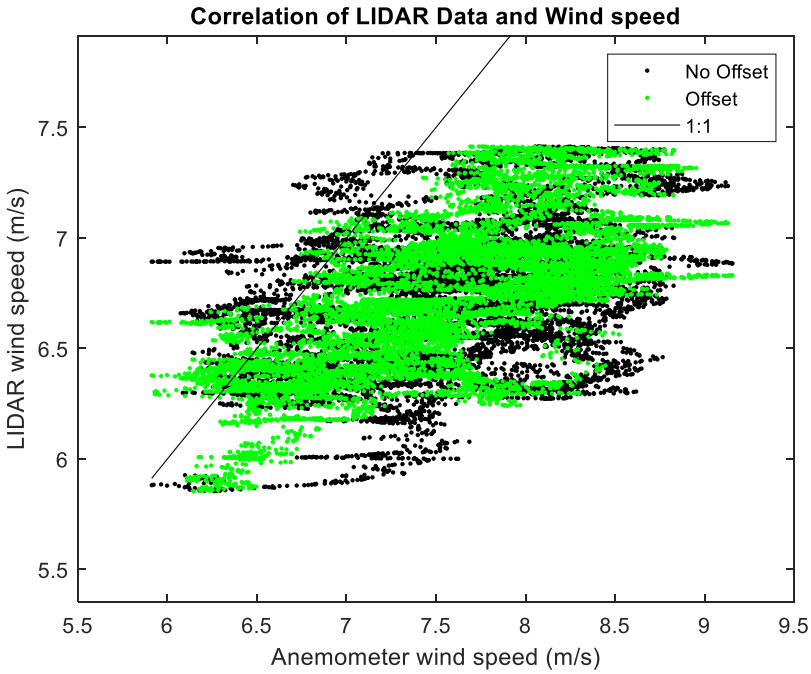

Figure 35 - Correlation before and after the time series offset

The blade loads will be positively correlated with wind speed below rated speed, as shown in Figure 36 (in which the time offset is 17.9s). It is interesting that the time offset is longer than it was for the anemometer wind speed – we can speculate that this is because inertial effects mean that the blade response lags behind the loading (the blade first flap natural frequency is 0.498Hz). The correlation coefficient is also better at 0.55 than it was for the anemometer wind speed (0.46).

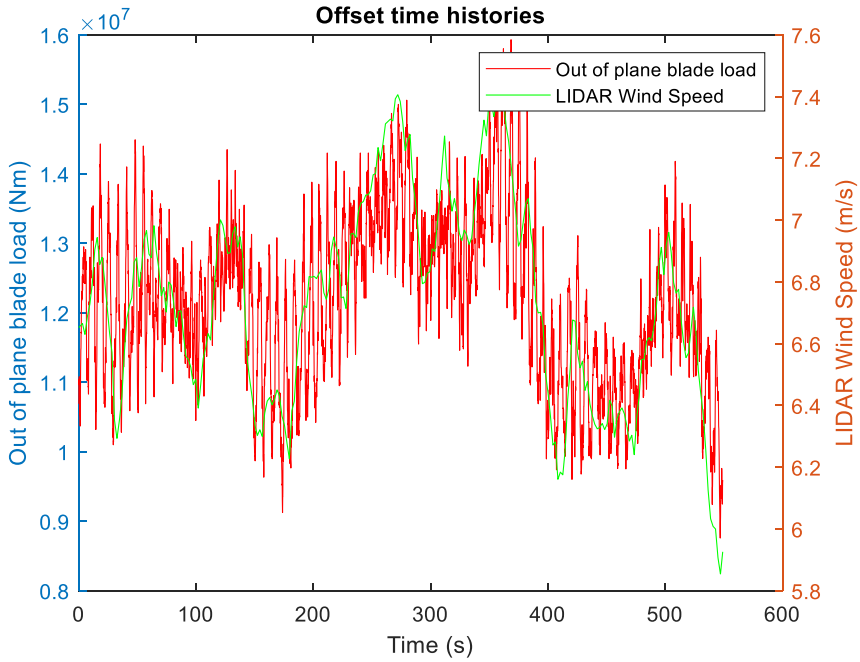

Figure 36 - Offset of 17.9s between LiDAR wind speed and blade load signal

This project has received funding from the European Union's Horizon 2020 Research and Innovation Programme under grant agreement No. 727680

Case 2

For Case 2, the expected advection time is 8.9s (112m at 12.6m/s). The method here gives an advection time of 9.2s with a correlation coefficient of 0.56, resulting in the time series comparison shown in Figure 37. The same exercise as before has been performed for the blade loads – again, the time lag is longer and correlation higher (10.4s and 0.78 respectively). As the turbine is operating just above rated power in this instance, the correlation between blade loads and LiDAR wind speed is now negative.

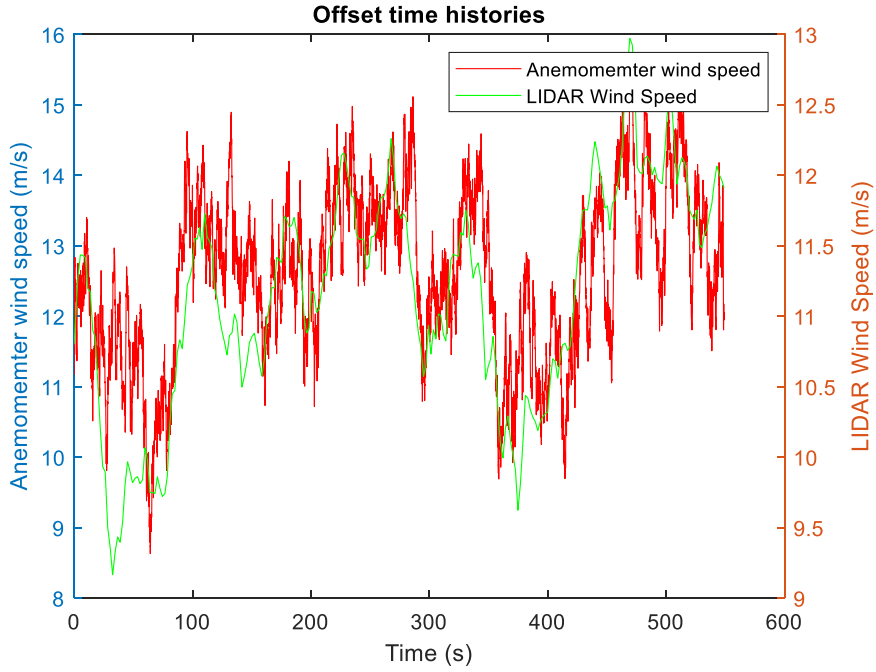

Figure 37 - Offset time histories for case 2

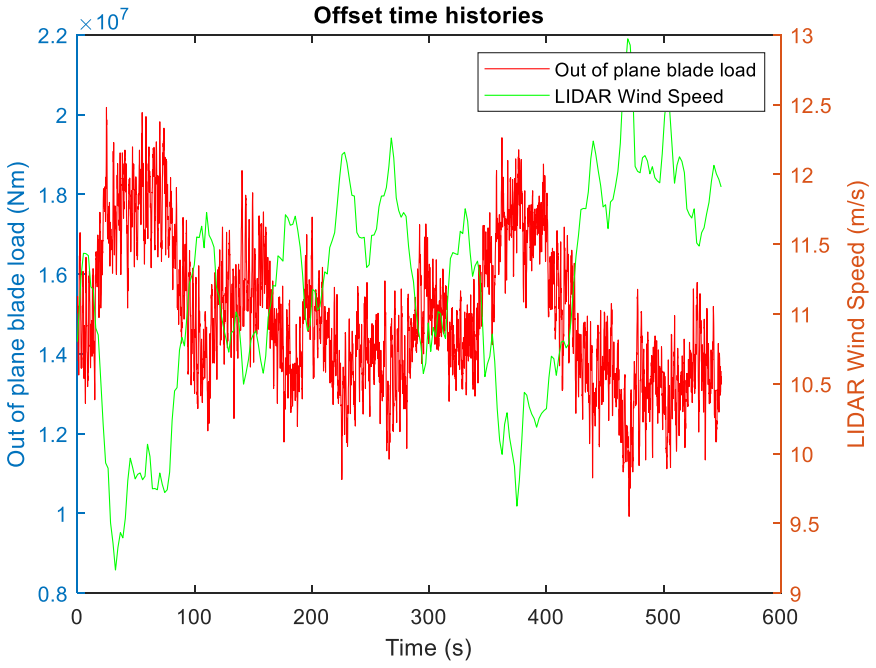

Figure 38 - Offset time histories of blade loads

This project has received funding from the European Union's Horizon 2020 Research and Innovation Programme under grant agreement No. 727680

Case 3

In this case, the turbine is operating well above rated power in an 18m/s wind speed. For the wind speed the expected advection time is 112m/17.98m/s, which is 6.2s. For this case, the advection time obtained by maximising the correlation is lower than that obtained by simple calculation – 4.95s with a correlation coefficient of 0.69 (the correlation coefficient appears to increase at higher wind speeds as well).

For the blade loads, the advection time is 7.85s with a correlation coefficient of 0.4236. All plots for this exercise follow this appendix.

Case 4

The higher turbulence intensity results in the turbine dropping well below rated power several times during the simulation as shown in Figure 39.

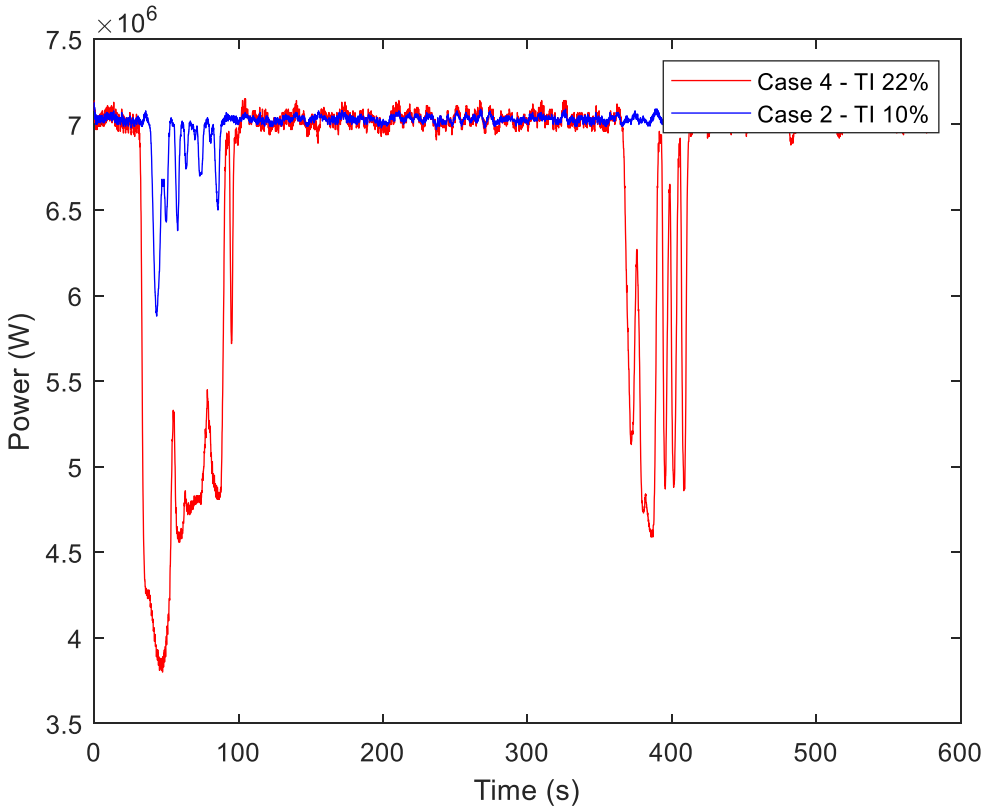

Figure 39 - Power production at different turbulence intensities

This means that the blade loads do not correlate as well, because below rated the loads are positively correlated and above they are negatively correlated. This can be seen in Figure 40. For case 4, the advection time based on blade loads is 11.25s with correlation coefficient of 0.34, and for wind speed it is 9.4s with correlation coefficient 0.55.

This project has received funding from the European Union's Horizon 2020 Research and Innovation Programme under grant agreement No. 727680

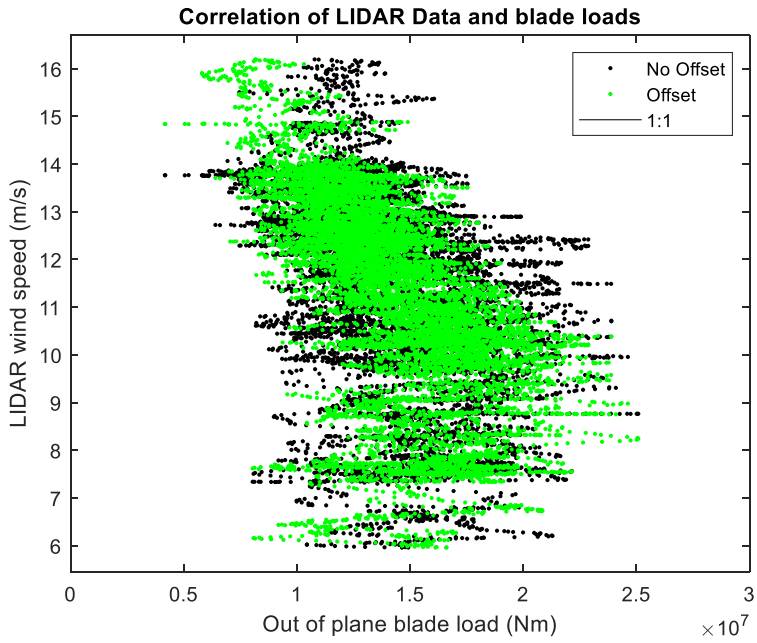

Figure 40 - Correlation of blade loads with LiDAR wind speed for Case 4

Case 5

For case 5, the advection time based on blade loads is 11.05s with correlation coefficient of 0.34, and for wind speed it is 9.4s with correlation coefficient 0.55.

For case 5, some other comparisons were performed. Bladed can output the rotor averaged wind speed, so this was compared with the LiDAR readings as shown in Figure 41. The offset time is 7.9s in this case, and the correlation coefficient is very high at 0.9724. The LiDAR reading is still lower than rotor plane wind speed, even when rotor averaging has been accounted for as shown in Figure 42. It is not clear why this is the case.

This project has received funding from the European Union's Horizon 2020 Research and Innovation Programme under grant agreement No. 727680

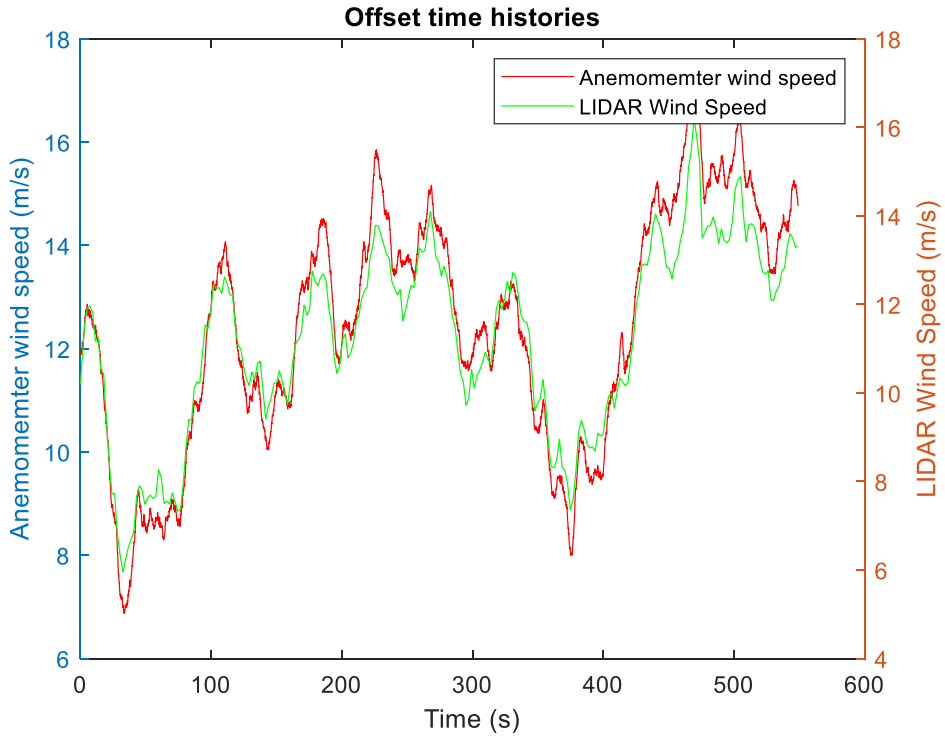

Figure 41 - Comparison of LiDAR reading with rotor average wind speed

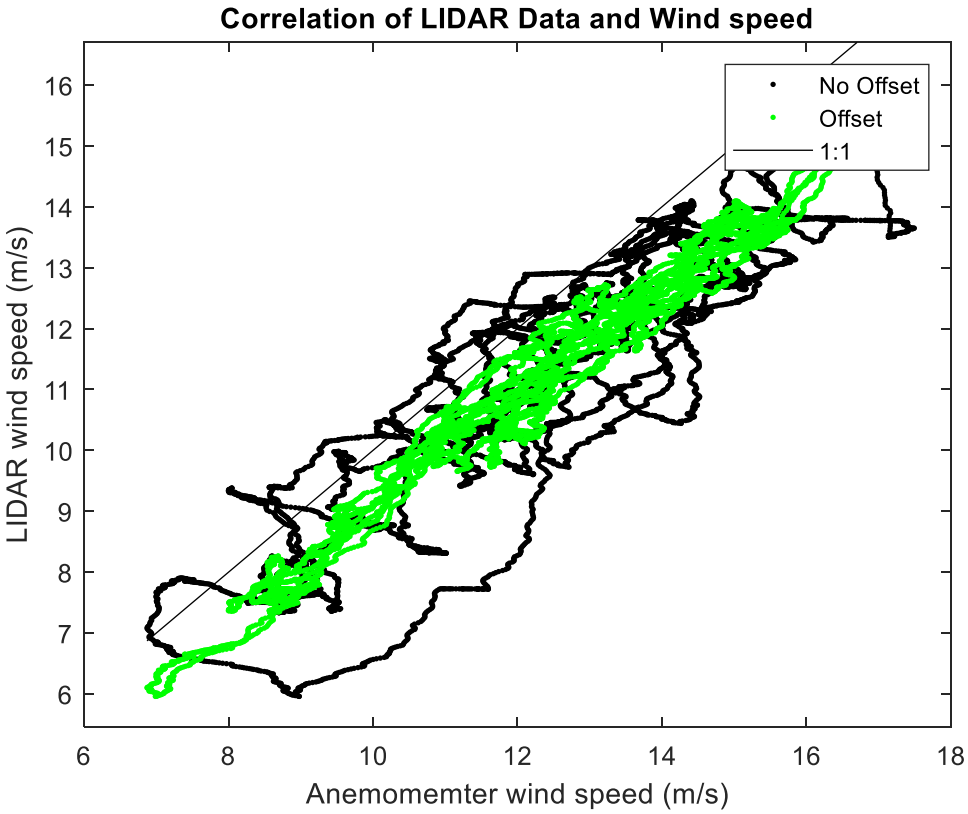

Figure 42 - Correlation of LiDAR with rotor average wind speed

This project has received funding from the European Union's Horizon 2020 Research and Innovation Programme under grant agreement No. 727680

The next case to be considered was to shrink the LiDAR scan area down to just the very centre of the rotor and change the sampling frequency to be the same as the simulation time step, but still using the evolving turbulence model so that the high frequency turbulence changes before it arrives at the turbine. This takes out the volume averaging effect and gives an advection time of 9s with correlation coefficient of 0.83. This is very close to the expected advection time of 9s, which indicates that time averaging may be shifting the data, and raises the question of when is the appropriate time in the scan to take as representative of the scan – we had initially assumed the middle of the scan.

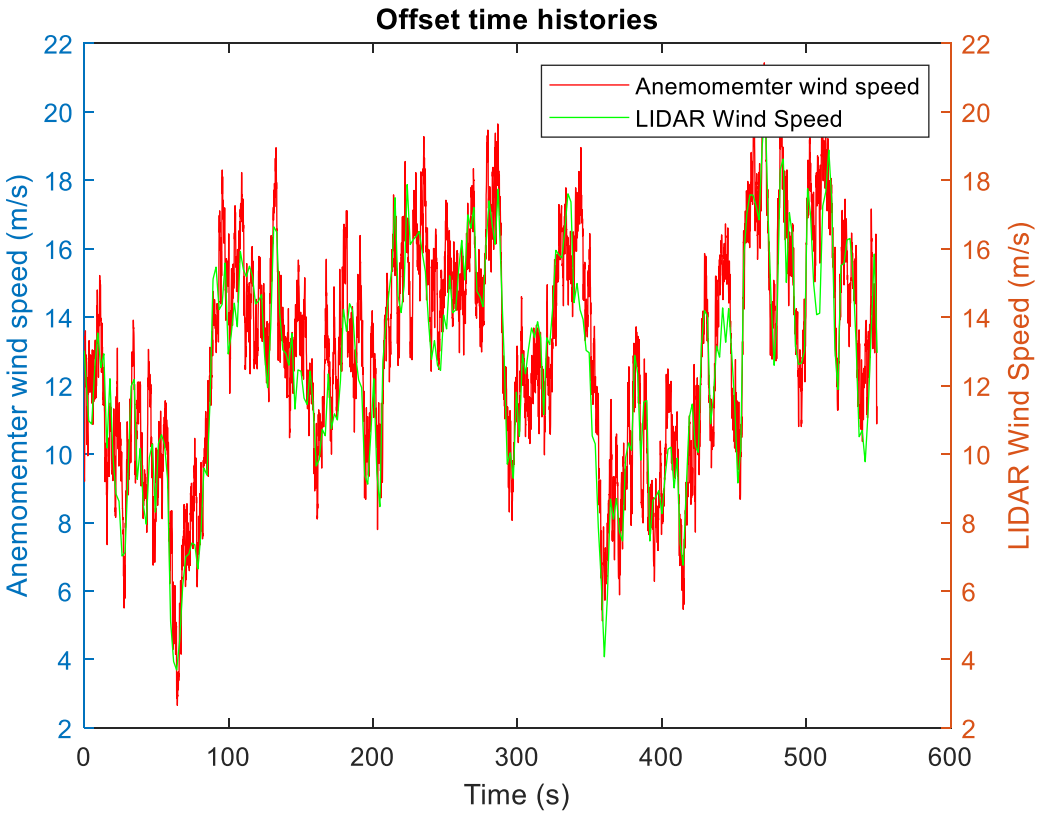

Figure 43 - Case 5 with LiDAR only scanning area ahead of hub centre (evolving turbulence model)

This project has received funding from the European Union's Horizon 2020 Research and Innovation Programme under grant agreement No. 727680

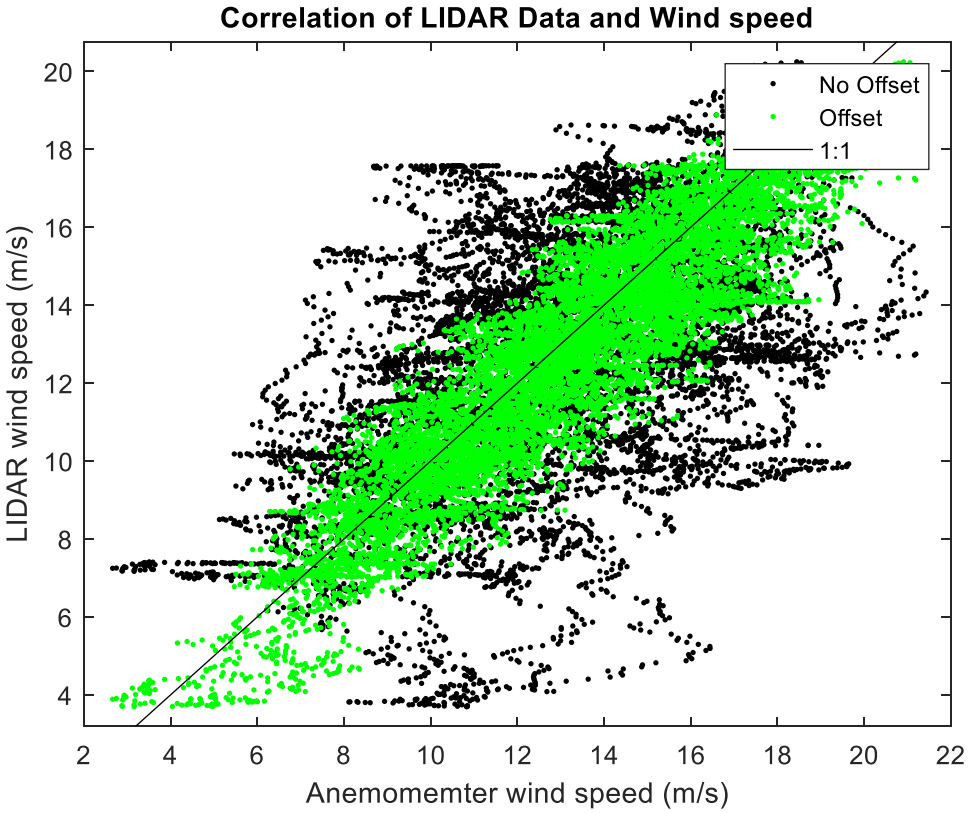

Figure 44 - Correlation of LiDAR data with anemometer for single scan point at the hub centre

Finally, we removed evolving turbulence and compared the results. This would be expected to give the best correlation, and it does – the advection time 9.05s (expected is 8.96s) and the correlation coefficient is 0.875.

Summary

A range of wind speeds and turbulence intensities have been studied using Bladed. As Bladed does not account for induction, this source of uncertainty around the advection time is removed, so we can isolate other parameters which effect the estimated advection time such as the volume averaging and time averaging effect of the LiDAR. We can also remove these effects by scanning a single point at the time step of the simulation. Using the blade loads as a proxy for the wind speed when determining the advection time by maximising correlation appears to be unwise – if the turbine is changing between below and above rated settings then the blade loads will be positively and negatively correlated, so poor correlation is guaranteed. Also, there appears to be a time lag related to the inertial response time of the blades which further confounds the results.

Table 7 shows a summary of the results obtained during this exercise. The last 3 cases, in which sources of uncertainty are removed one-by-one, are quite instructive – they appear to indicate that the time averaging has some impact on the advection time. For the LiDAR wind speed, the representative time for each scan was chosen as the middle of the step, but this does not necessarily seem to be correct. Case 5A, in which the rotor average wind speed (which is volume but not time averaged) is compared to a LiDAR scan taking 2.1s (which is time and volume averaged) has very high correlation but the time lag is lower by around half of the time averaging

This project has received funding from the European Union's Horizon 2020 Research and Innovation Programme under grant agreement No. 727680

period, whereas for the last two cases where the LiDAR is forced to take a single scan point at the same measurement interval as the simulation time step has exactly the expected advection time.

Table 7 - Summary of advection times determined by maximising correlation

Case	Wind Speed	Turbulence Intensity	Expected Advection Time	Advection Time (Wind Speed)	Corr. Coef.	Advection Time (Blade Loads)	Corr. Coef.
	[m/s]	[%]	[s]	[s]	[-]	[s]	[-]
1	7.54	10.00	14.85	15.65	0.46	17.90	0.57
1A	7.47	10.00	14.99	14.50	0.94	-	-
2	12.60	10.00	8.89	9.20	0.56	10.50	0.78
2A	12.39	10.00	9.04	7.85	0.97	-	-
3	17.98	10.00	6.23	4.90	0.69	7.85	0.42
3A	17.71	10.00	6.32	5.55	0.97	-	-
4	12.96	22.00	8.64	9.40	0.55	11.25	0.34
4A	12.43	22.00	9.01	7.9	0.97	-	-
5	12.96	27.00	8.64	9.40	0.55	11.05	0.34
5A	12.45	27.00	9.00	7.90	0.97	-	-
5B	12.96	27.00	8.64	9.00	0.83	-	-
5C	12.96	27.00	8.64	9.05	0.88	-	-

In order to assess why this occurs, the rotor averaged case was compared for cases 1-3 to give a range of average wind speeds (Cases 1A, 2A, 3A, 4A and 5A). All these cases have very high correlation coefficients and faster advection than would be expected if the wind field is just being moved along at the mean wind speed.

Figure 45 shows fits of the advection time to the inverse wind speed (the inverse wind speed has been used to allow a linear fit to be used). For both the rotor averaged wind speed and the anemometer wind speed there is a time offset, which is probably related to the time averaging effect of the LiDAR.

This project has received funding from the European Union's Horizon 2020 Research and Innovation Programme under grant agreement No. 727680

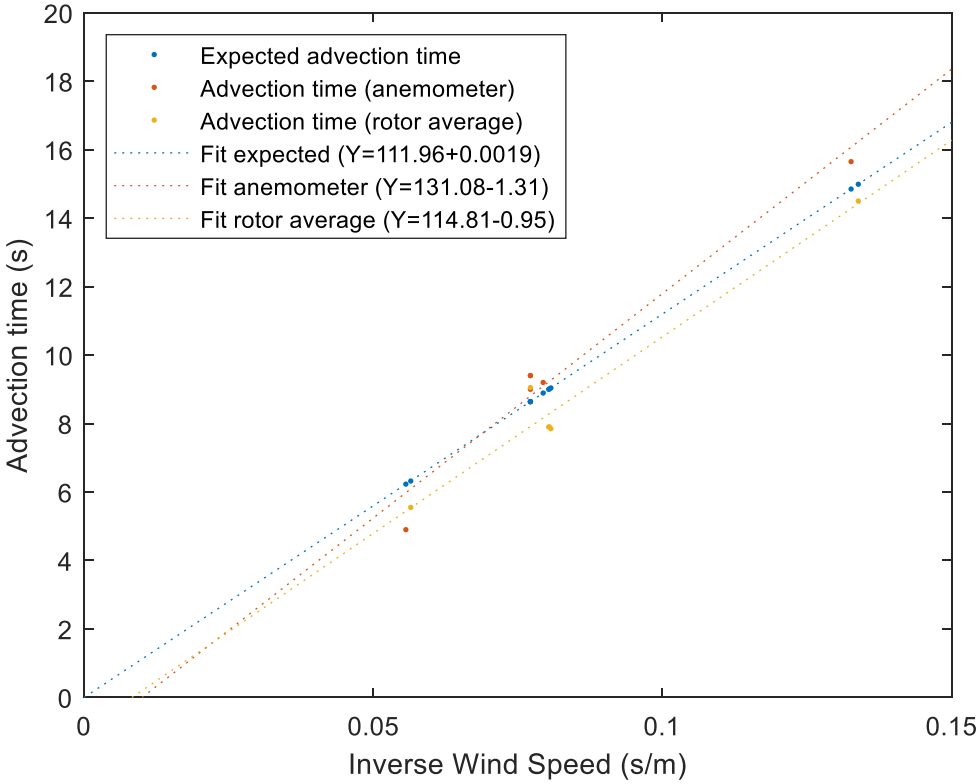

Figure 45 - Advection time against inverse wind speed for studied load cases

This project has received funding from the European Union's Horizon 2020 Research and Innovation Programme under grant agreement No. 727680

Case 1 – Wind Speed: 7.5m/s TI: 10% Evolving Turbulence

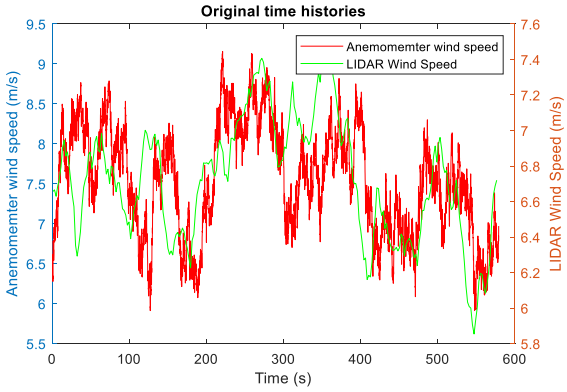

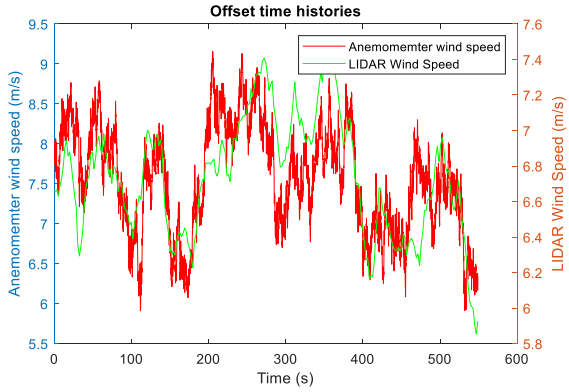

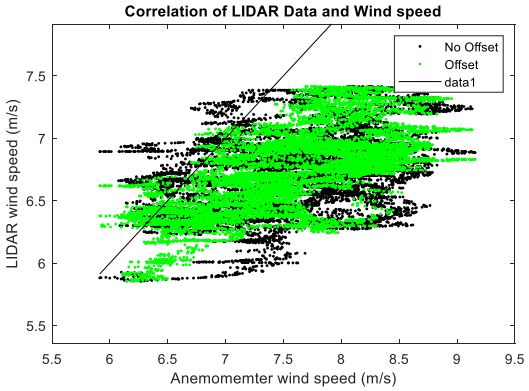

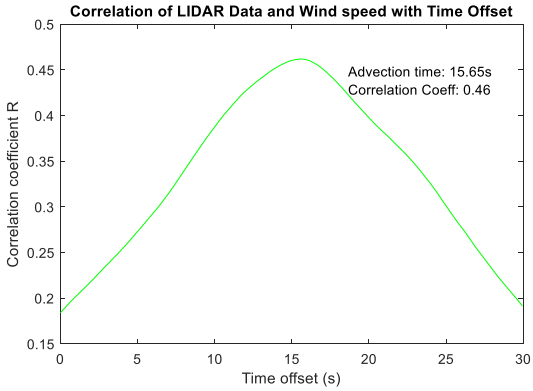

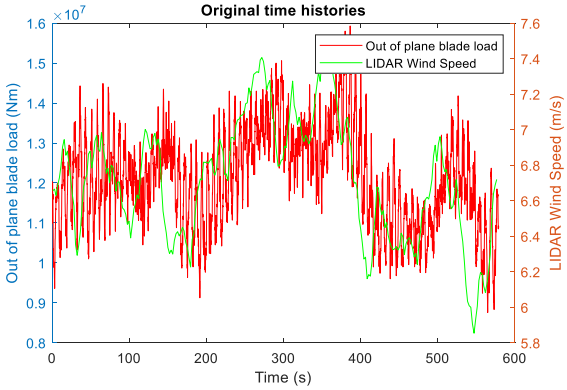

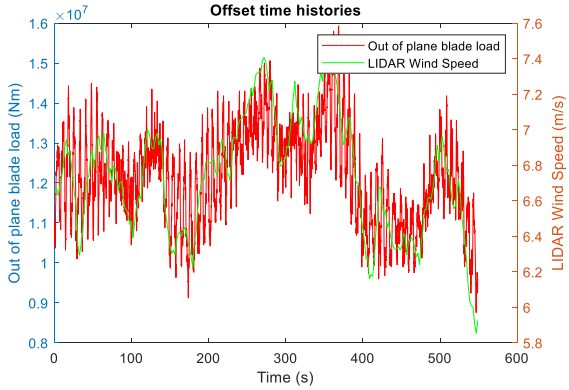

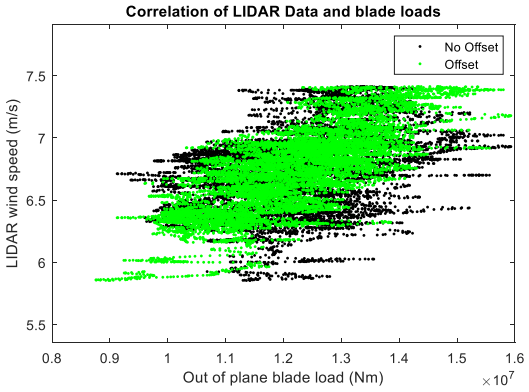

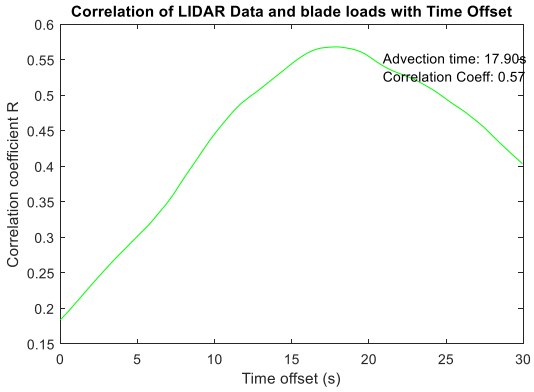

This project has received funding from the European Union's Horizon 2020 Research and Innovation Programme under grant agreement No. 727680

Case 2 – Wind Speed 12.5m/s TI: 10% Evolving Turbulence

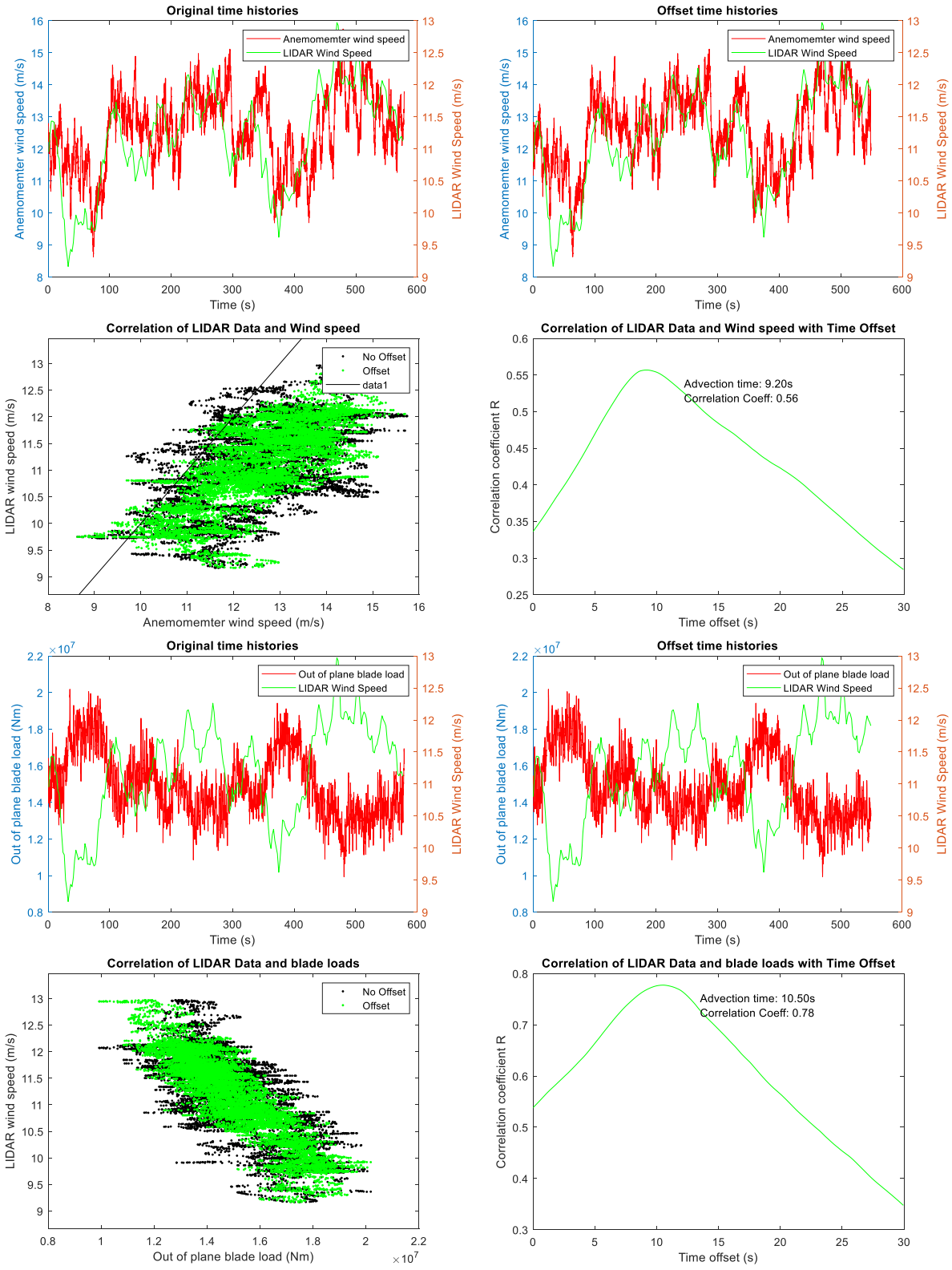

This project has received funding from the European Union's Horizon 2020 Research and Innovation Programme under grant agreement No. 727680

Case 3 – Wind Speed: 18m/s TI: 10% Evolving Turbulence

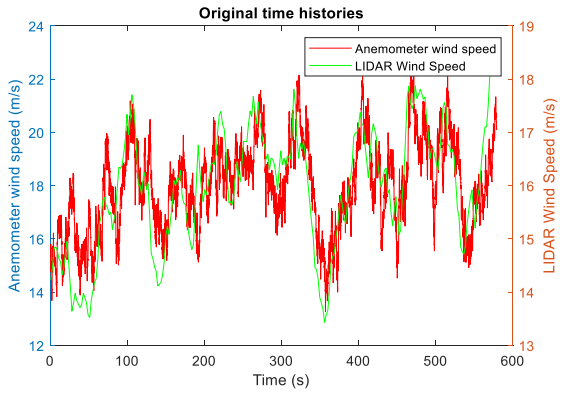

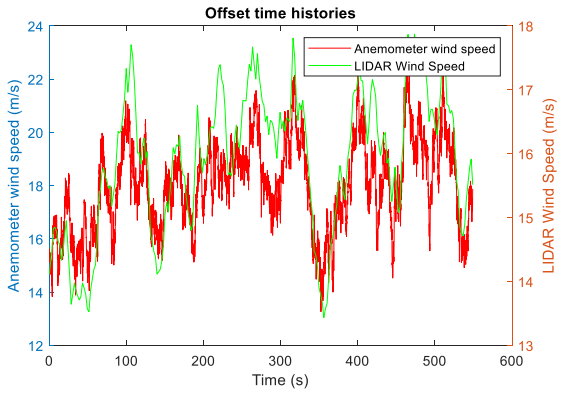

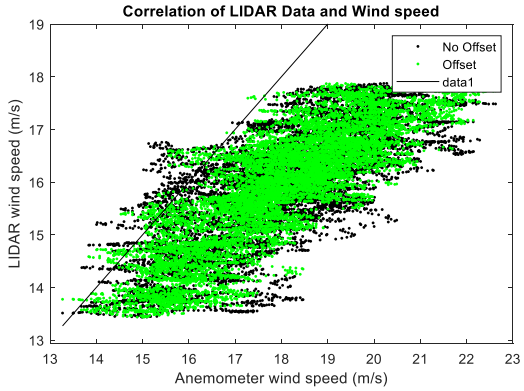

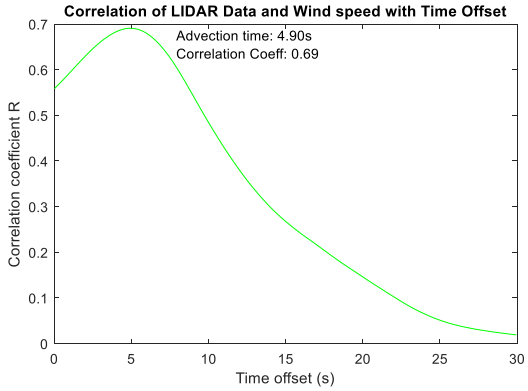

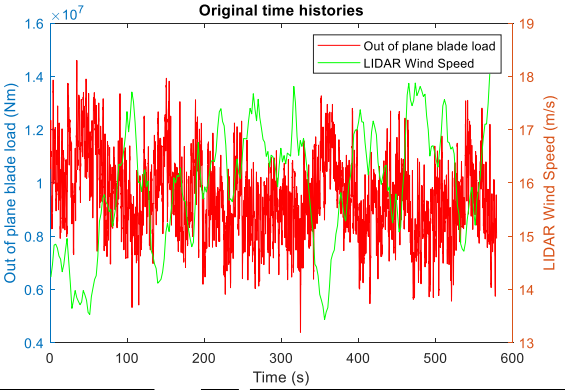

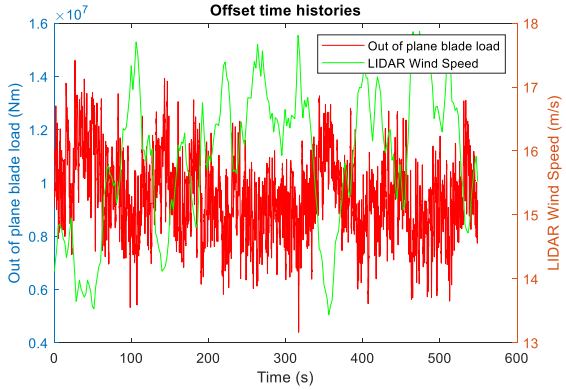

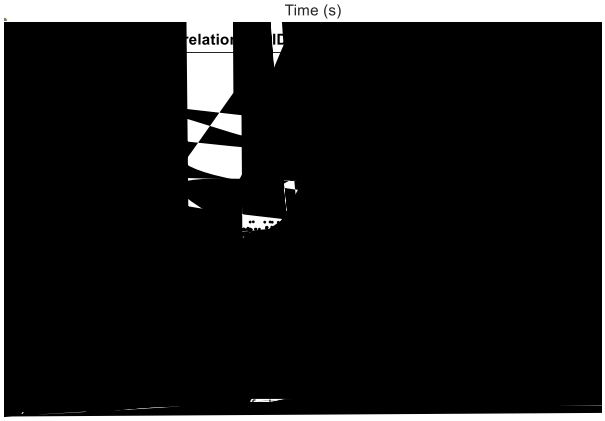

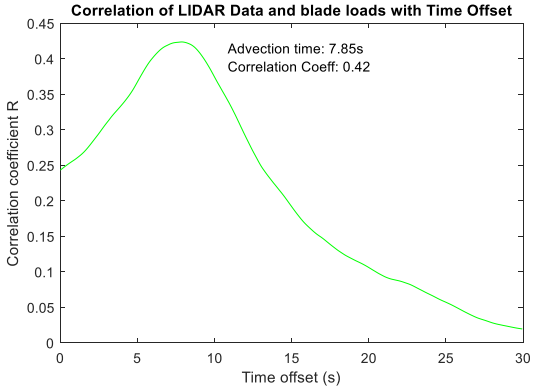

This project has received funding from the European Union's Horizon 2020 Research and Innovation Programme under grant agreement No. 727680

Case 4 – Wind Speed: 12.5m/s TI: 22% Evolving Turbulence

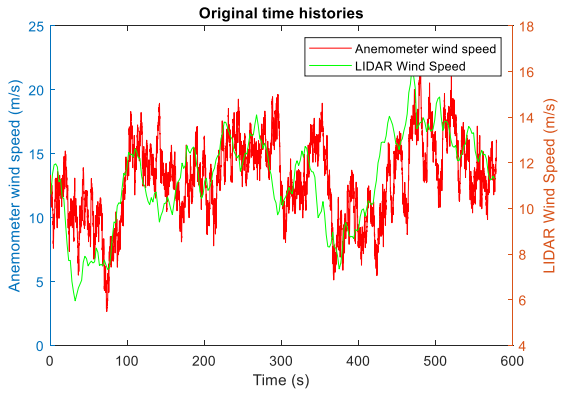

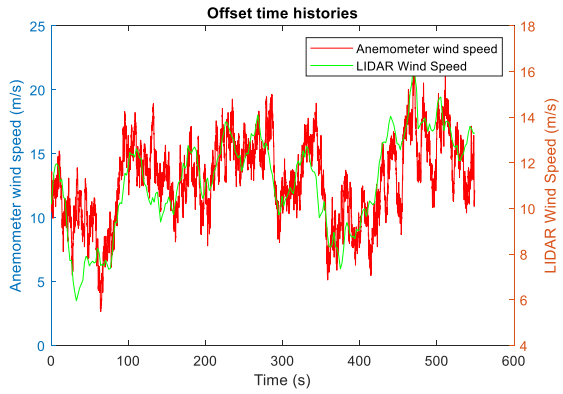

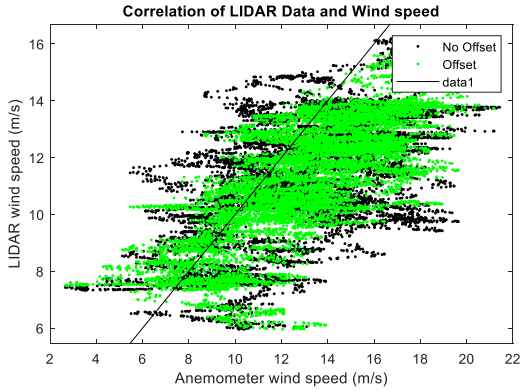

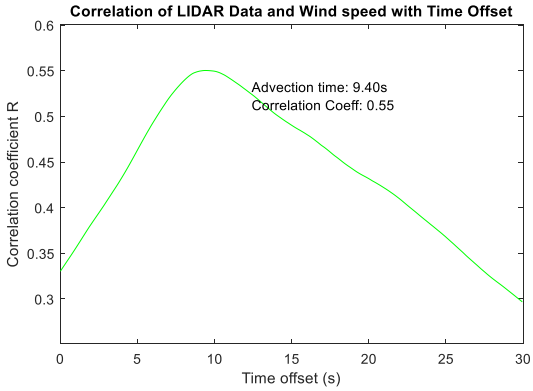

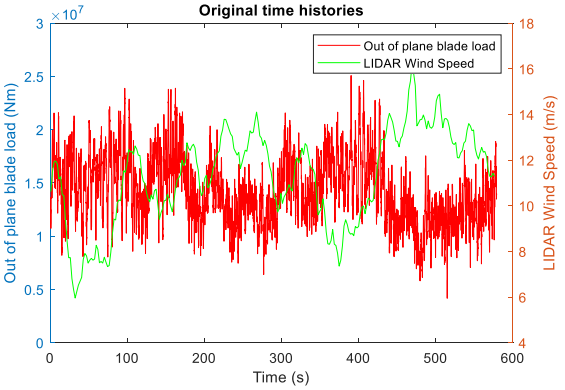

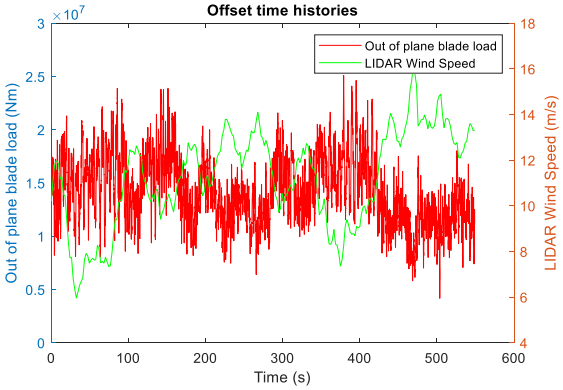

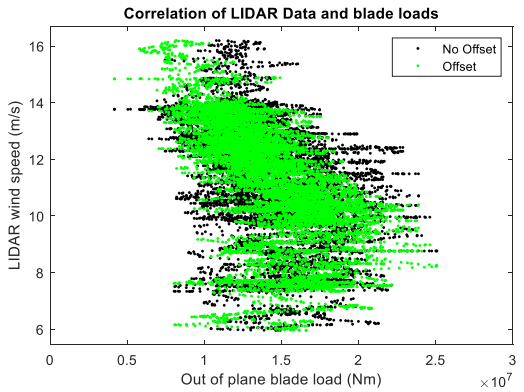

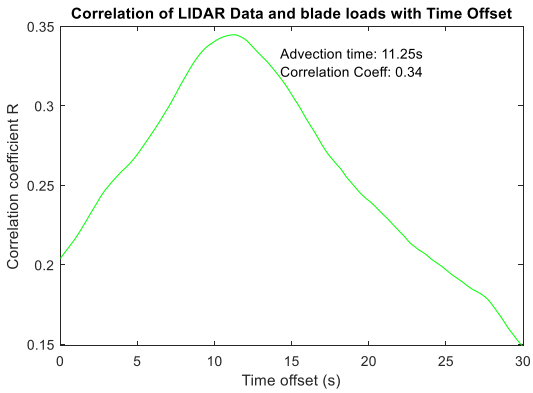

This project has received funding from the European Union's Horizon 2020 Research and Innovation Programme under grant agreement No. 727680

Case 5 – Wind Speed: 12.5m/s TI: 27% Evolving Turbulence

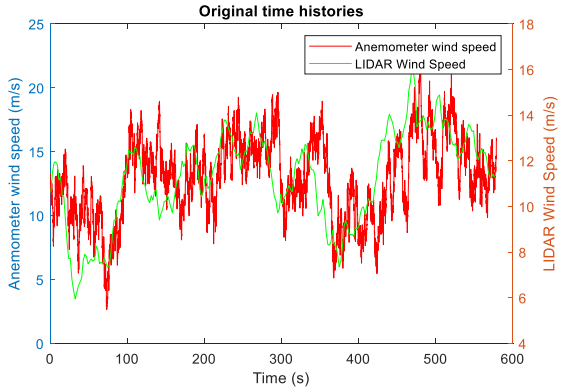

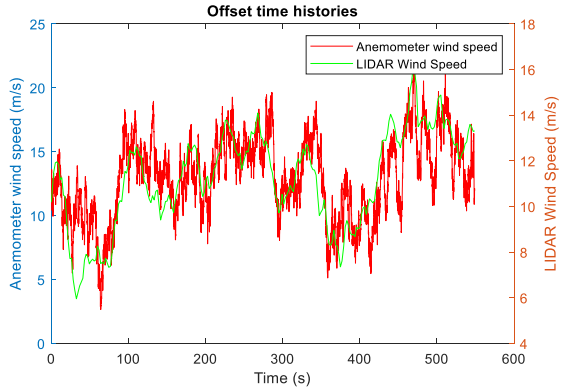

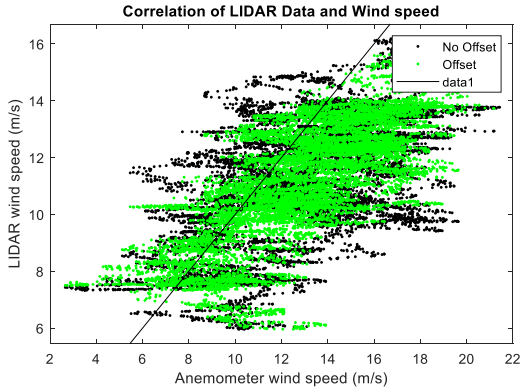

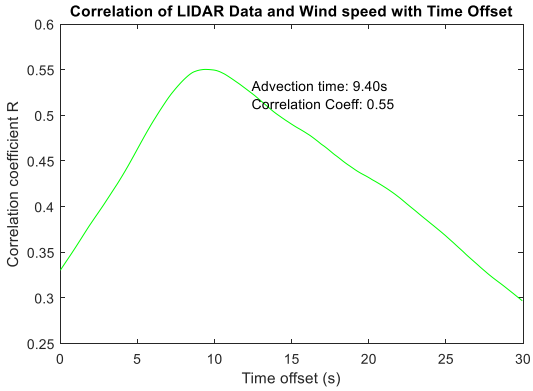

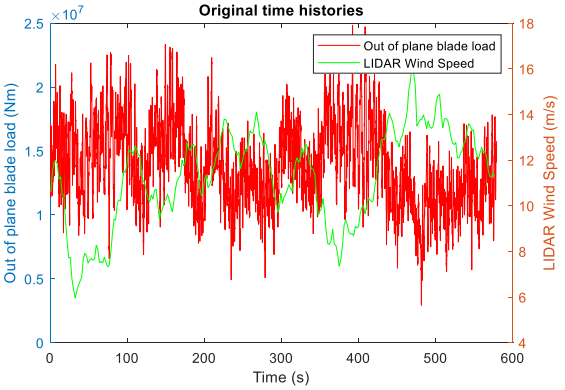

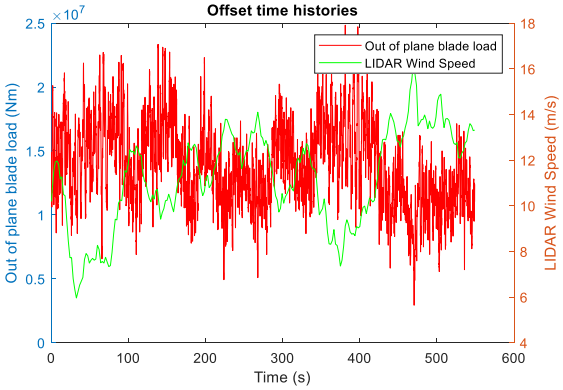

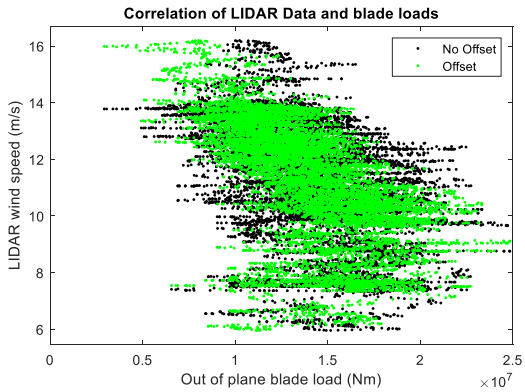

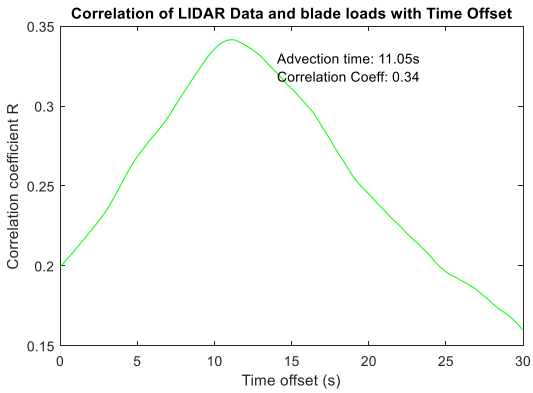

This project has received funding from the European Union's Horizon 2020 Research and Innovation Programme under grant agreement No. 727680

Case 5A – As Case 5 but using rotor average wind speed

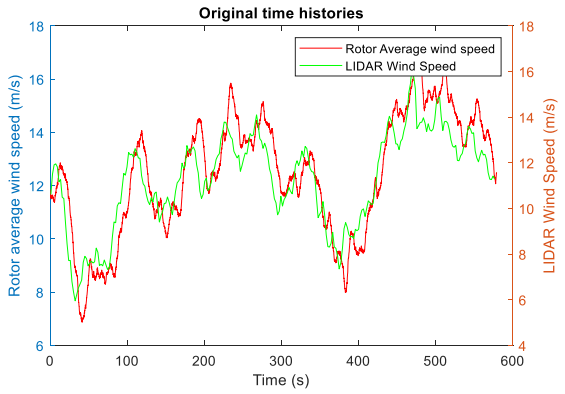

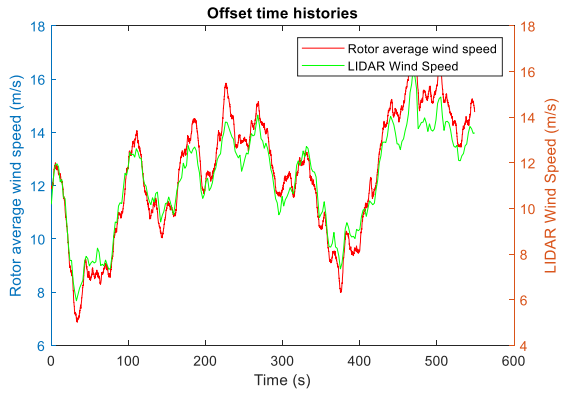

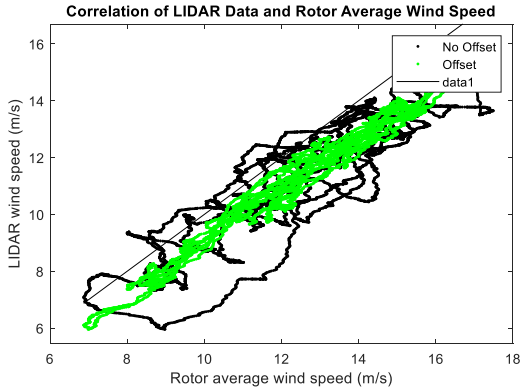

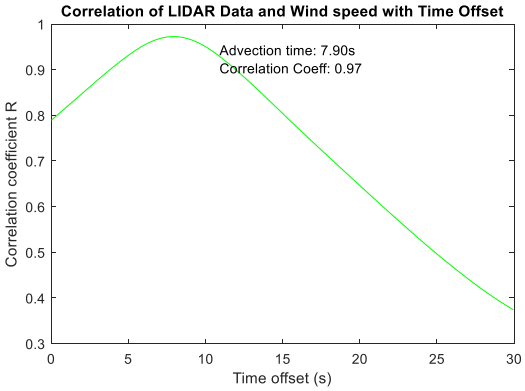

Case 5B – As Case 5 but using single LiDAR scan point

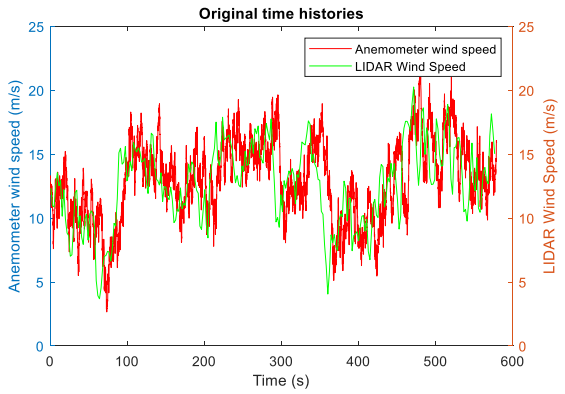

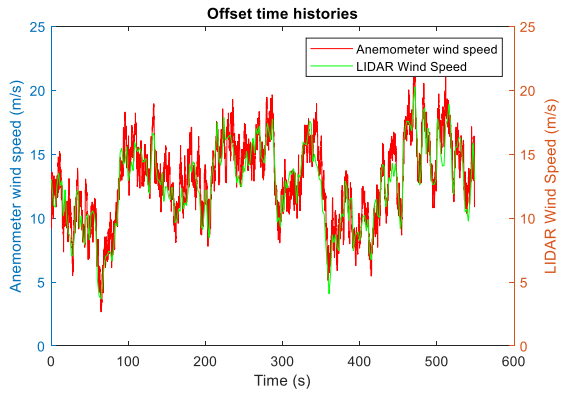

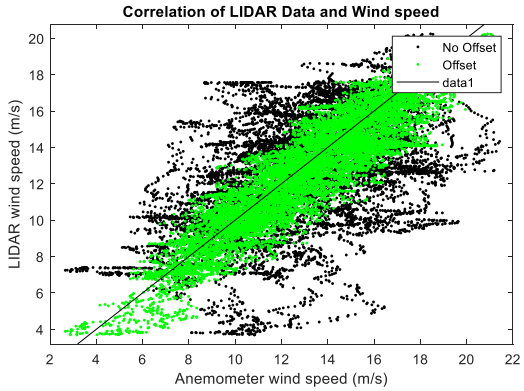

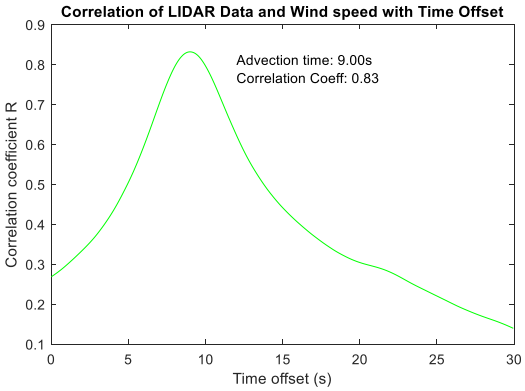

This project has received funding from the European Union's Horizon 2020 Research and Innovation Programme under grant agreement No. 727680

Case 5C – As Case 5 but using single LiDAR scan point and frozen turbulence

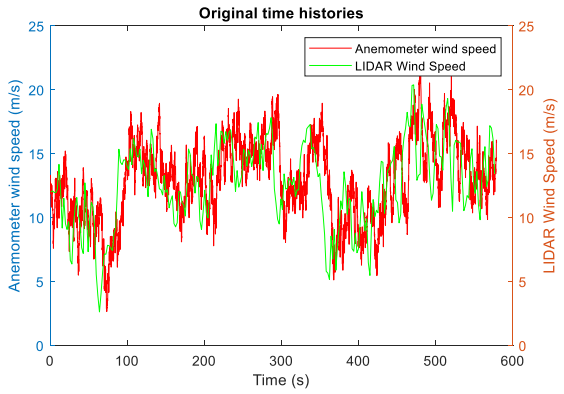

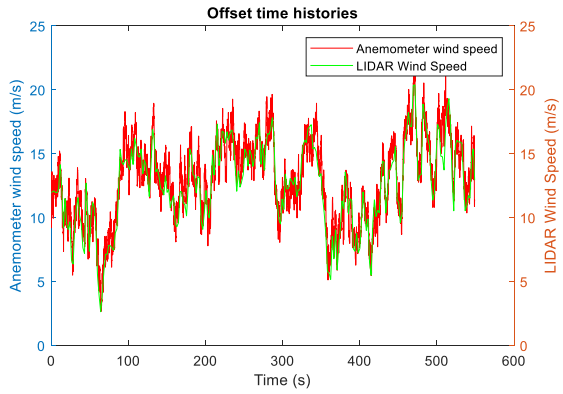

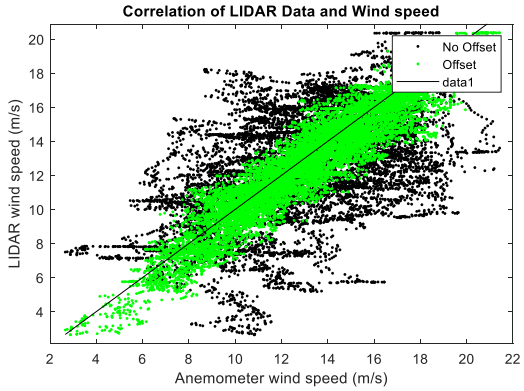

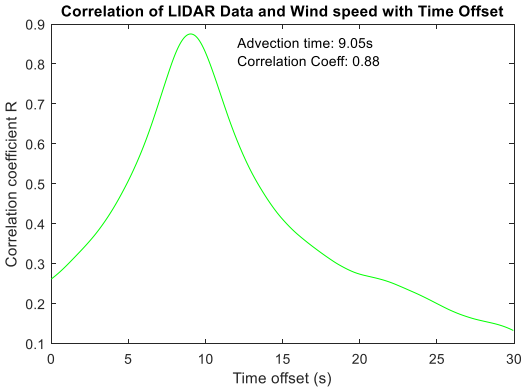

This project has received funding from the European Union's Horizon 2020 Research and Innovation Programme under grant agreement No. 727680